DRUG DISCOVERY

Network pharmacology-based assessment of anti-inflammatory action of phytocompounds derived from *Nigella sativa* and *Moringa oleifera*

Funmilayo ID Afolayan*, **Christopher T Tarkaa**

To Cite:
Afolayan FID, Tarkaa CT. Network pharmacology-based assessment of anti-inflammatory action of phytocompounds derived from *Nigella sativa* and *Moringa oleifera*. *Drug Discovery* 2023; 17: e13dd1016
doi: https://doi.org/10.54905/disssi.v17i39.e13dd1016

Author Affiliation:
Cell Biology and Genetics, Department of Zoology, University of Ibadan, Ibadan, Nigeria

***Corresponding Author**
Cell Biology and Genetics, Department of Zoology, University of Ibadan, Ibadan
Nigeria
Email: fidifede@gmail.com

Peer-Review History
Received: 03 January 2023
Reviewed & Revised: 06/January/2023 to 03/March/2023
Accepted: 07 March 2023
Published: 12 March 2023

Peer-Review Model
External peer-review was done through double-blind method.

Drug Discovery
pISSN 2278–540X; eISSN 2278–5396

DISCOVERY SCIENTIFIC SOCIETY

ABSTRACT

Studies have shown that *Nigella sativa* and *Moringa oleifera* possess anti-inflammatory activity, however, the molecular targets involved in their mechanisms of action are not known. A network-based pharmacology analysis was done to predict molecular targets and phytocompounds involved in the anti-inflammatory activity of *N. sativa* and *M. oleifera*. Phytocompounds of *N. sativa* and *M. oleifera* were retrieved from Dr Duke's Phytochemical and Ethnobotanical databases and Indian Medicinal Plants, Phytochemistry and Therapeutics database. Target proteins were obtained from Binding DB. A compound-target-pathway network was constructed with the Cytoscape tool and a network of protein-protein interactions was established with the STRING database. Lead proteins identified from the compound-target-pathway network were further studied for their interactions with *N. sativa* and *M. oleifera* by molecular docking. Similarly, biological pathways involved in the anti-inflammatory activity of the phytocompounds were identified with the Kyoto Encyclopedia of Genes and Genomes (KEGG) analysis. Forty-two and twenty-seven bioactive compounds from *N. sativa* and *M. oleifera* respectively were successfully identified corresponding to 98 targets that were screened out for anti-inflammation. Based on network pharmacology data and molecular docking, beta-sitosterone, astragalin, beta-amyrin and quercetin were predicted to inhibit key inflammatory proteins. Target proteins, including NR1H3, F2, AKT1, HSP90AA1, IL2, NFKB1, PTGS2, ALOX5, TNF-α, IL6 and IFN-γ, as well as signaling pathways such as TNF, MAPK, IL-17 and HIF-1 were linked to the anti-inflammatory activity of *N. sativa* and *Moringa oleifera.* Functional enrichment analysis predicted that 33 inflammatory pathways were modulated by *N. sativa* and *M. oleifera* which need further analyses for confirmation.

Keywords: *Nigella sativa*, *Moringa oleifera*, Anti-inflammation, In silico, Network Pharmacology

1. INTRODUCTION

Inflammation is the body's defense mechanism that eliminates injurious stimuli such as irritants, damaged cells, infection and other stimulants and initiates the process of healing (Jain et al., 2015). Acute inflammation, with exudation of fluid and plasma proteins at the affected site, intravascular activation of platelets and the emigration leukocytes as its main characteristics occurs very fast and the process can last for a few minutes to numerous days. Chronic inflammation on the other hand occurs when acute inflammation occurs repeatedly or continuously, with the process lasting for several weeks to months and even years (Kosala et al., 2018; Kumar et al., 2018). Inflammation is like a two-edged sword because although it removes injurious stimuli and initiates the healing process, dysregulated inflammation can lead to tissue and cell injury, chronic infection, chronic diseases and cancers (Roth, 2012). Some drugs are presently used to manage inflammatory conditions. These drugs include steroidal anti-inflammatory drugs (SAIDs) and non-steroidal anti-inflammatory drugs (NSAIDs). Non-steroidal anti-inflammatory drugs remain a mainstay of therapy for the treatment of a large number of inflammatory diseases. Non-steroidal anti-inflammatory drugs do not cure the disease but instead modify the inflammatory response to the disease. The use of NSAIDs is frequently limited by gastrointestinal side effects, that range from dyspepsia to bleeding from ulceration which can be life-threatening. Non-steroidal anti-inflammatory drugs have been reported to inhibit the cyclooxygenase (COX) pathway (Borquaye et al., 2020).

Cyclooxygenase is required for the conversion of arachidonic acid to prostaglandins, prostacyclin and thromboxanes. Specifically, prostaglandin causes vasodilation, increases the temperature set-point in the hypothalamus and play a role in anti-nociception, prostacyclins cause vasodilation, inhibition of platelet aggregation, relaxation of gastrointestinal and uterine muscle and release of pituitary hormones and thromboxane plays a role in platelet adhesion (Jain et al., 2015; Ghlichloo and Gerriets, 2021). Two cyclooxygenase isoenzymes, cyclooxygenase-1 (COX-1) and cyclooxygenase-2 (COX-2) are known. Cyclooxygenase-1 is constitutively expressed in the body, and it plays an important role in the maintenance of gastrointestinal mucosa lining, kidney function and platelet aggregation. Cyclooxygenase-2 is not constitutively expressed in the body, rather, it is expressed during an inflammatory response. The Majority of the NSAIDs are nonselective and are known to inhibit both COX-1 and COX-2. A few NSAIDs such as celecoxib and refecoxib are selective and can target only COX-2, thus having a different side effect profile (Ghlichloo and Gerriets, 2021). Other side effects of anti-inflammatory drugs include gastric ulcers, gastric irritation, alterations in renal function, hepatic injury, effects on blood pressure and platelet inhibition which may result in increased bleeding (Geremew et al., 2015). It is therefore imperative to develop newer anti-inflammatory drugs that are safer for use by humans.

Traditional medicines have been used for ages to maintain health and improve various diseases including chronic inflammatory diseases. These agents comprise various plant sources and are associated with minimal side effects (compared to modern allopathic medicines), show synergistic effects by interacting with multiple proteins and modulating multiple pathways (Yuan et al., 2017). About 25% of medicines used today are developed from traditionally used medicines; however, there is a paucity of scientific evidence for the mechanism of multicomponent treatments (Duyu et al., 2020). *Nigella sativa* is a plant that belongs to the family Ranunculaceae and it is an annual herbaceous plant that is native to Southern Europe, Southwest Asia and North Africa. The plant is commonly known as black cumin and it is cultivated in many countries including South Europe, India, Syria, Turkey, Pakistan, the Middle Eastern Mediterranean region and Saudi Arabia (Hannan et al., 2021). *N. sativa* has been studied extensively for its biological activities and therapeutic potential and shown to possess a wide spectrum of activities such as diuretic, antihypertensive, anticancer, anti-inflammatory, antidiabetic, immunomodulatory, anthelmintic, antimicrobial, hepatoprotective, renal protective, gastroprotective, spasmolytic, bronchodilator and antioxidant activities (Kooti et al., 2016).

Moringa oleifera is a plant that belongs to the family Moringaceae and it is a small tree of the sub-Himalayan region of North West India, that is now indigenous to many regions in Africa, South East Asia, Arabia, the Caribbean and Pacific Islands and South America. The plant is commonly known as moringa and it is widely used for its health benefits. Among commoners, it has earned its name as the miracle tree because of its amazing healing abilities for various ailments (Razis et al., 2014). Each part of the plant (fruits, seeds, leaves, flowers, bark and roots) has one or more benefits and are being used traditionally for different purposes, making it one of the most used plants in the world today (Mallenakuppe et al., 2019). *M. oleifera* has also been studied extensively for its biological activities and therapeutic potential and has also shown to possess a wide spectrum of activities such as antidiabetic, anticonvulsant, antidepressant, anti-inflammatory, anticancer, immunomodulatory, antihyperlipidemic, antimicrobial, antiulcer, antiarthritic, antioxidant, SCAR marker, antimutagenic, antifungal, antiurolithiatic activities (Srivastava et al., 2020).

Network pharmacology is a research field that uses several components and several targets as the starting point, to study the molecular mechanism of action of various drugs and plants in the treatment of diseases (Zhang et al., 2020). This method integrates system biology, multiple pharmacology and computer analysis technology. Unlike the previous concept of single-component/single target, network pharmacology uses a large number of databases and statistical algorithms to identify the synergistic effects of

several components, several targets and several pathways of disease (Yu et al., 2020). It also explores the interaction between the drugs and potential targets and establishes a "compounds-targets-pathways" network to associate drugs systematically and comprehensively (Xie et al., 2015). Network pharmacology is thus a more holistic approach in carrying out research than the single-component/single-target approach.

Molecular docking is usually used to validate the interactions between the compounds and target (Que et al., 2021). Molecular docking is a high-throughput technology that is widely applied to study the active sites of drugs by simulating interactions between receptors and drug molecules (Yu et al., 2020). It has therefore played an immense role in the research of natural products (Gogoi et al., 2017). In this study, network pharmacology was used to construct the active components-targets-pathways network diagram of phytocompounds present in *Nigella sativa* and *Moringa oleifera.* Additionally, molecular docking technology was used to predict the potential active components and mechanism of action of the plants. These findings set the basis for further research in this direction.

2. MATERIALS AND METHODS

Collection of Active Components

The reported phytoconstituents from *Nigella sativa* and *Moringa oleifera* were retrieved from Dr Duke's Phytochemical and Ethnobotanical Database (DPED) (https://phytochem.nal.usda.gov/phytochem/search) and Indian Medical Plants, Phytochemistry and Therapeutics (IMPPAT) (https://cb.imsc.res.in/imppat/home) using the keywords *"Nigella sativa"* and *"Moringa oleifera"* respectively (Gu et al., 2013). Canonical SMILES of each compound along with their molecular weight and the molecular formula were recorded from PubChem (https://pubchem.ncbi.nlm.nih.gov/) and Chemspider (https://www.chemspider.com/) databases (Kim et al., 2015).

Prediction and Screening of the Inflammatory Targets of the Active Components

The targets of each compound were queried using Binding DB (https://www.bindingdb.org/) at a percentage similarity of 70%. The gene code of each target was identified using UniProt (https://www.uniprot.org/). Similarly, targets for inflammation were identified with reference to the Gene Cards database (https://www.genecards.org/) (Zhang et al., 2020).

Drug likeness and ADMET Profile

The drug-likeness score for each compound targeting proteins related to inflammation was predicted using the Mol Soft database (https://molsoft.com/) based on *"Lipinski's Rule of Five"* model (Duyu et al., 2020). Likewise, the probability for human intestinal absorption, caco-2 and blood-brain barrier permeability, human oral bioavailability, P-glycogen substrate, P-glycoprotein, CYP3A4, CYP2C9, CYP2D6 and CYP1A2 inhibition, eye irritation, Ames mutagenesis, human ethera-go-go inhibition, carcinogenicity, hepatotoxicity, etc. were predicted using admetSAR2.0 (http://lmmd.ecust.edu.cn/admetsar2/) (Yang et al., 2019).

Pathway Enrichment Analysis

The potential gene targets were uploaded to the KOBAS 3.0 database (http://kobas.cbi.pku.edu.cn/kobas3) for KEGG pathway annotation. These enriched pathways were considered significant ones that will be affected by *Nigella sativa* and *Moringa oleifera* in the treatment of inflammation (Yu et al., 2020).

Construction of Protein-Protein Interaction Network

The gene targets were imported into the STRING database (https://string-db.org/) to generate the target protein interaction network. The TSV file was downloaded and imported into Cytoscape 3.8.2 software and the network was analyzed using the Network Analysis function (Ye et al., 2020).

Construction of components–targets–pathways network

The active components, gene targets and enrichment pathways were imported into the Cytoscape 3.8.2 software to construct the components-targets-pathways network. Active components, gene targets and enrichment pathways represent the input nodes. The association between the 2 nodes is represented by an edge (Yu et al., 2020).

Molecular Docking

Based on the network pharmacological outcome, molecular docking analyses were carried out between the phytoconstituents and AKT1 and HSP90AA1 (the proteins that interact with most targets) and NR1H3 and F2 (the proteins that are targeted by most

phytoconstituents). Because IL-2, NFKB1, PTGS2 (COX-2), ALOX5, TNF, IL-6 and IFN-γ are closely linked to inflammation, they were also subjected to docking studies (Yu et al., 2020). The 3D structures of the proteins were obtained from the protein data bank (https://www.rcsb.org/). The PDB ID of AKT1, HSP90AA1, NR1H3, F2, IL-2, NFKB1, PTGS2, ALOX5, TNF-α and IL-6 are 1UNR, 3OWB, 2ACL, 1PPB, 1M47, 1A3Q, 5IKT, 3O8Y, 1TNF, 1ALU and 1FG9 respectively. To avoid docking interference, heteroatoms and water molecules were removed with discovery studio 2021 (Duyu et al., 2020) and hydrogen bonds were added using Chimera 1.14 (Johnson et al., 2020). The active sites of the proteins were obtained from the CASTp 3.0 database (http://sts.bioe.uic.edu/castp/) (Tian et al., 2018). The SDF (structure-data file) structures of the phytoconstituents and standard ligand i.e., diclofenac was obtained from the PubChem database. The ligands were docked to the protein targets at their active sites and the binding affinities were determined using Auto dock Vina from PyRx. Molecular interactions between proteins and ligands were viewed with Chimera 1.14 and discovery studio 2021 (Johnson et al., 2020).

3. RESULTS

Active components and their targets

Eighty-one (81) phytoconstituents were identified from *N. sativa,* out of which forty-two (42) were associated with inflammation (Table 1). Also, fifty-seven (57) were identified from *M. oleifera* in which twenty-seven (27) modulated proteins involved in inflammation (Table 2). Diclofenac was chosen as the standard drug because it is one of the common non-steroidal anti-inflammatory drugs used in the treatment of inflammation and pain (Kolodziejska and Kolodziejczyk, 2018).

Drug-likeness and ADMET profile

Out of Forty-two phytoconstituents from *N. sativa*, twenty-one phytoconstituents were predicted to score positive and negative drug-likeness hit each. Similarly, out of twenty-seven compounds from *M. oleifera*, seventeen and ten were predicted to score positive and negative drug likeness hit respectively. Rutin was predicted to score the highest drug-likeness score of 0.91 for *N. sativa* while delta-5-avenasterol was predicted to score the highest drug likeness score of 0.85 for *M. oleifera*.

Twenty-four phytoconstituents from *N. sativa* were predicted to violate 1 Lipinski rule, two phytoconstituents (Caspase 8 inhibitor and Quercetin-3′-glucoside) were predicted to violate 2 Lipinski rules and one phytoconstituent (Rutin) was predicted to violate three Lipinski rules. Fourteen phytoconstituents from *M. oleifera* were predicted to violate one Lipinski rule and one compound (Maltotriose) was predicted violate three Lipinski rules.

The list of phytoconstituents and drug likeness scores are summarized in tables 3 and 4. The ADMET profile of each phytoconstituent is represented in the heat maps (Figures 1 and 2). All the phytoconstituents from *N. sativa* are predicted to have positive human intestinal absorption scores. All the phytoconstituents from *N. sativa* except Astragalin, Betulic acid, Hederagenin, Quercetin-3′-glucoside and Rutin are blood-brain barrier permeants, twenty-two phytoconstituents have positive bioavailability scores and all phytoconstituents apart from Caspase 8 inhibitor and Carvacrol are predicted to be non-inhibitors of P-glycogen. Caspase 8 inhibitor, Dithymoquinone and Nigellone are predicted to be inhibitors of CYP3A4 and nine phytoconstituents are predicted to be inhibitors of CYP1A2. Twelve phytoconstituents are predicted to cause eye irritation. Astragalin, Butyrospermol, Quercetin-3′-glucoside and Rutin are predicted to be mutagenic, eight phytoconstituents are predicted to be inhibitors of human ether a-go-go, eight phytoconstituents showed a tendency towards hepatotoxicity and none of the phytoconstituents showed a tendency towards carcinogenicity.

Table 1 Phytoconstituents of *Nigella sativa* and the inflammatory proteins they target

S/N	Phytoconstituents	Targets
1	24-ethyl-lophenol	PRKAB1, CACNA1C, F7, F10, GRIN2B, GRIN1, ITGB3, PTPRC, ELANE, NFKB1, RORC, NR1H3, NR1H2, PTPN1, F2
2	24-methylene-cycloartanol	NR1H3
3	24-methyl-lophenol	PRKAB1, CACNA1C, F7, F10, GRIN2B, GRIN1, ITGB3, PTPRC, ELANE, NFKB1, RORC, NR1H3, NR1H2, PTPN1, F2
4	5-dehydro-avenasterol	CYP24A1, GRIN2B, GRIN1, ITGB3, RORC, NR1H3, NR1H2, F2, RXRA
5	Alpha-spinasterol	PRKAB1, CACNA1C, F10, GRIN2B, GRIN1, ITGB3 RORC, NR1H3, NR1H2, PTPN1, F2
6	Astragalin	ALOX5, IL2, MMP9, NOX4, PTPN1, F2, RPS6KA3, TNF

7	Beta-amyrin	F7, F10, GRIN2B, GRIN1, ITGB3, PTPRC, ELANE, NFKB1, RORC, NR1H3, NR1H2, PTPN1, F2
8	Betulic acid	F7
9	Butyrospermol	PRKAB1, CACNA1C, F7, F10, GRIN2B, GRIN1, ITGB3, PTPRC, ELANE, NFKB1, RORC, NR1H3, NR1H2, PTPN1, F2
10	Campesterol	PRKAB1, F10, GRIN2B, GRIN1, ITGB3, RORC, NR1H3, NR1H2, PTPN1, F2
11	Carvacrol	ATP2A1
12	Carvone	BIRC2
13	Caspase 8 Inhibitor	ACE, CAPN2, CAPN1, CASP3, CASP7, CASP8, CASP9, CTSK, CTSS, ITGA2B, ITGB3, ELANE, MALT1, PSEN1, CTSL, REN, CMA1
14	Caspase inhibitor VI	CAPN2, CAPN1, CASP3, CASP7, CASP8, CASP9, CTSK, CTSS, NFKBIA, ITGA2B, ITGB3, ELANE, MALT1, PSEN1, CTSL
15	Cholesterol	PRKAB1, F10, GRIN2B, GRIN1, ITGB3, RORC, NR1H3, NR1H2, PTPN1, F2
16	Citrostadienol	PRKAB1, CACNA1C, F7, F10, GRIN2B, GRIN1, ITGB3, PTPRC, ELANE, NFKB1, RORC, NR1H3, NR1H2, PTPN1, F2
17	Cycloeucalenol	NR1H3
18	Damascenine	ALOX5
19	Dehydroascorbic-acid	ALOX5
20	Delta 7-avenasterol	PRKAB1, CACNA1C, F10, GRIN2B, GRIN1, ITGB3 RORC, NR1H3, NR1H2, PTPN1, F2
21	Dithymoquinone	BIRC2
22	Dl-alanine-15n	GRIN1
23	Eicosadienoic-acid	PTPN7, PPARA
24	Gramisterol	PRKAB1, CACNA1C, F7, F10, GRIN2B, GRIN1, ITGB3, PTPRC, ELANE, NFKB1, RORC, NR1H3, NR1H2, PTPN1, F2
25	Hederagenin	F7, F10, PTPRC, ELANE, NOS2, NFKB1, RORC, NR1H3, PPARA, PTGS2, PTPN1
26	Indole-3-acetic-acid	C5, PTGS2
27	Lophenol	PRKAB1, CACNA1C, F7, F10, GRIN2B, GRIN1, ITGB3, PTPRC, ELANE, NFKB1, RORC, NR1H3, NR1H2, PTPN1, F2
28	N-acetyl-L-cysteine	ACE
29	Nigellone	BIRC2
30	Obtusifoliol	CACNA1C, F10, GRIN2B, GRIN1, ITGB3, RORC, NR1H3, NR1H2, PTPN1, F2
31	Octadeca-9,12-dienoic acid	PTPN7, PPARA
32	Oleic acid	PTPN7, PPARA
33	Phytosterols	PRKAB1, F10, GRIN2B, GRIN1, ITGB3, RORC, NR1H3, NR1H2, PTPN1, F2
34	Quercetin-3'-glucoside	ALOX5, IL2, MMP9, NOX4, PTPN1, F2, RPS6KA3, TXNRD1, TNF
35	Rutin	ALOX5, IL2, MMP9, NOX4, PTPN1, F2, RPS6KA3, TXNRD1, TNF
36	Stigmast-7-en-3-beta-ol	PRKAB1, CACNA1C, F10, GRIN2B, GRIN1, ITGB3, RORC, NR1H3, NR1H2, PTPN1, F2
37	Stigmastanol	RORA, NR1H3

38	Taraxerol	F7, F10, GRIN2B, GRIN1, ITGB3, PTPRC, ELANE, NFKB1, RORC, NR1H3, NR1H2, PTPN1, F2
39	Thymohydroquinone	ATP2A1
40	Thymol	ALOX5, ATP2A1
41	Thymoquinone	ALOX5
42	Tirucallol	CACNA1C, F10, GRIN2B, GRIN1, ITGB3, RORC, NR1H3, NR1H2, PTPN1, F2
43	*Diclofenac	CXCR1, PTGS2, CXCL8

*Standard drug

Table 2 Phytoconstituents of *Moringa oleifera* and the Inflammatory proteins they target

S/N	Phytoconstituents	Targets
1	24-Methylene-cholesterol	CACNA1C, HSP90AA1, BIRC2, NR1H3
2	28-Isoavenasterol acetate	RORC, F10, PTPN1, NR1H2, NR1H3
3	4-hydroxymellein	IL6, PRKCA
4	Benzyl-amine	F2, F10
5	Beta-sitosterone	CACNA1C, HSP90AA1, BIRC2, NR1H3
6	Brassicasterol	ITGB3, F2, GRIN2B, PRKAB1, GRIN1, RORC, F10, PTPN1, NR1H2, NR1H3
7	Caffeic-acid	LCK, MMP2, MMP1, MMP9, EGFR
8	Campestanol	RORA, NR1H3
9	Campesterol	PRKAB1, F10, GRIN2B, GRIN1, ITGB3, RORC, NR1H3, NR1H2, PTPN1, F2
10	Clerosterol	PRKAB1, F10, GRIN2B, GRIN1, ITGB3, RORC, NR1H3, NR1H2, PTPN1, F2
11	Delta-5-avenasterol	PRKAB1, F10, GRIN2B, GRIN1, ITGB3, RORC, NR1H3, NR1H2, PTPN1, F2
12	Delta-7-avenasterol	PRKAB1, F10, GRIN2B, GRIN1, ITGB3, RORC, NR1H3, NR1H2, PTPN1, F2, CACNA1C
13	Delta-tocopherol	PTGS2, NDUFA4, AKT1, ALOX5, PPARA, GSTP1, PTGER3
14	D-galactose	HDAC1, ABL1, HDAC10, VEGFA, FGF2, ABL2, HDAC3, HDAC2, CDK2, HDAC9, HDAC6, HDAC4, FGF1, CDK1, HDAC8
15	Dl-alanine-15n	GRIN1
16	Dl-arginine	NOS3, NOS2
17	D-xylose	HDAC1, ABL1, HDAC10, VEGFA, FGF2, ABL2, HDAC3, HDAC2, HDAC9, HDAC6, HDAC4, HDAC5, FGF1, HDAC8
18	Gamma-tocopherol	PTGS2, AKT1, PTGER4, ALOX5, PPARA, GSTP1, PTGER3
19	Indole-3-acetic-acid	C5, PTGS2
20	Indoleacetonitrile	MPO, AHR
21	Kaempferol	PGF, PTGS2, IGF1R, BACE1, F2, LCK, MET, FLT3, VEGFA, TERT, GSK3B, ALOX5, EGFR, PIK3CG, CDK6, PPARA, CSNK2A1, YP1B1, PTPN1, NOX4, AHR, CDK2, NTRK2, CDK5, PIM1, CDK1, KIT, ABCC1
22	L-rhamnose	HDAC1, ABL1, HDAC10, VEGFA, FGF2, ABL2, HDAC3, HDAC2, CDK2, HDAC9, HDAC6, HDAC4, FGF1, CDK1, HDAC8
23	Maltotriose	HDAC1, PRKCA, ABL1, HDAC10, VEGFA, FGF2, ABL2, HDAC3, HDAC2, CDK2, HDAC9, HDAC6, HDAC4, HDAC5, FGF1, CDK1, HDAC8

24	Phytosterols	PRKAB1, F10, GRIN2B, GRIN1, ITGB3, RORC, NR1H3, NR1H2, PTPN1, F2
25	Quercetin	PGF, PTGS2, IGF1R, BACE1, F2, LCK, MET, FLT3, VEGFA, TERT, GSK3B, ALOX5, EGFR, PIK3CG, CDK6, PPARA, CSNK2A1, YP1B1, PTPN1, NOX4, AHR, CDK2, NTRK2, CDK5, PIM1, CDK1, KIT, ABCC1
26	Stigmastanol	RORA, NR1H3
27	Vanillin	ERN1
28	*Diclofenac	CXCR1, PTGS2, CXCL8

*Standard drug

Table 3 The molecular formula, physicochemical properties and drug-likeness scores of phytoconstituents from *N. sativa*

Compounds	Molecular formula	Molecular mass (g/mol)	NHBA	NHBD	MolLogP	DLS
24-ethyl-lophenol	$C_{30}H_{52}O$	428.40	1	1	8.24	0.40
24-methylene-cycloartanol	$C_{31}H_{52}O$	440.40	1	1	8.49	-0.48
24-methyl-lophenol	$C_{29}H_{50}O$	414.39	1	1	7.79	0.17
5-dehydro-avenasterol	$C_{29}H_{46}O$	410.35	1	1	7.34	0.57
Alpha-spinasterol	$C_{29}H_{48}O$	412.37	1	1	7.87	-0.05
Astragalin	$C_{21}H_{20}O_{11}$	448.10	11	7	-0.12	0.67
Beta-amyrin	$C_{30}H_{50}O$	426.39	1	1	7.95	-0.22
Betulic acid	$C_{30}H_{48}O_3$	456.36	3	2	7.05	0.25
Butyrospermol	$C_{30}H_{50}O$	426.39	1	1	8.81	0.46
Campesterol	$C_{28}H_{48}O$	400.37	1	1	7.87	0.59
Carvacrol	$C_{10}H_{14}O$	150.10	1	1	3.44	-0.35
Carvone	$C_{10}H_{14}O$	150.1	1	0	2.99	-1.40
Caspase 8 inhibitor	$C_{30}H_{43}FN_{40}O_{11}$	654.29	11	5	1.72	-1.33
Caspase inhibitor VI	$C_{21}H_{28}FN_3O_7$	453.19	7	4	1.02	-1.58
Cholesterol	$C_{27}H_{46}O$	386.35	1	1	7.44	0.49
Citrostadienol	$C_{30}H_{50}O$	426.39	1	1	7.74	0.47
Cycloeucalenol	$C_{30}H_{50}O$	426.39	1	1	7.22	0.25
Diamascenine	$C_{10}H_{13}NO_3$	195.09	3	1	1.36	-0.86
Dehydroascorbic-acid	$C_6H_6O_6$	174.02	6	2	-1.95	-0.60
Delta 7-avenasterol	$C_{29}H_{48}O$	412.37	1	1	7.95	0.25
Dithymoquinone	$C_{20}H_{24}O_4$	328.17	4	0	2.76	-0.89
Dl-alanine-15N	$C_3H_7NO_2$	89.05	3	3	-2.64	-0.96
Eicosadienoic-acid	$C_{20}H_{36}O_2$	308.27	2	1	7.61	-0.30
Gramisterol	$C_{29}H_{48}O$	412.37	1	1	7.39	0.13
Hederagenin	$C_{30}H_{48}O_4$	472.36	4	3	4.99	0.47
Indole-3-acetic-acid	$C_{10}H_9NO_2$	175.06	2	2	1.62	-1.43
Lophenol	$C_{28}H_{48}O$	400.37	1	1	7.36	0.11
N-acetyl-L-cysteine	$C_5H_9NO_3S$	163.03	4	3	-0.92	0.30
Nigellone	$C_{20}H_{24}O_4$	328.17	4	0	2.76	-0.89
Obtusifoliol	$C_{30}H_{50}O$	426.39	1	1	7.38	0.85
Octadeca-9,12-dienoic acid	$C_{18}H_{32}O_2$	280.24	2	1	6.60	-0.30
Oleic acid	$C_{18}H_{34}O_2$	282.26	2	1	7.11	-0.30
Phytosterols	$C_{29}H_{50}O$	414.39	1	1	8.45	0.78
Quercetin-3'-glucoside	$C_{21}H_{20}O_{12}$	464.10	12	8	-0.54	0.68
Rutin	$C_{27}H_{30}O_{16}$	610.15	16	10	-1.55	0.91

Stigmast-7-en-3-beta-ol	$C_{29}H_{50}O$	414.39	1	1	8.58	0.18
Stigmastanol	$C_{29}H_{52}O$	416.40	1	1	8.83	0.22
Taraxerol	$C_{30}H_{50}O$	426.39	1	1	8.11	-0.90
Thymohydroquinone	$C_{10}H_{14}O_2$	166.10	2	2	2.34	-1.28
Thymol	$C_{10}H_{14}O$	150.10	1	1	3.43	-0.54
Thymoquinone	$C_{10}H_{12}O_2$	164.08	2	0	2.07	-1.03
Tirucallol	$C_{30}H_{50}O$	426.39	1	1	8.74	0.55
*Diclofenac	$C_{14}H_{11}Cl_2NO_2$	295.02	2	2	4.52	0.59

NHBA- Number of hydrogen bond acceptors, NHBD- Number of hydrogen bond donors, DLS- Drug-likeness score

Table 4 The molecular formula, physicochemical properties and drug-likeness scores of phytoconstituents from *M. oleifera*

Compounds	Molecular formula	Molecular mass (g/mol)	NHBA	NHBD	MolLogP	DLS
24-methylene-cholesterol	$C_{28}H_{46}O$	398.35	1	1	7.47	0.51
28-isoavenasterol acetate	$C_{32}H_{52}O_2$	468.40	2	0	8.25	1.20
4-hydroxymellein	$C_{10}H_{10}O_4$	194.06	4	2	1.31	-0.01
Benzyl-amine	C_7H_9N	107.07	1	2	1.04	-1.33
Beta-sitosterone	$C_{29}H_{48}O$	412.37	1	0	8.40	0.68
Brassicasterol	$C_{28}H_{46}O$	398.35	1	1	7.08	0.34
Caffeic-acid	$C_9H_8O_4$	180.08	4	3	1.27	-0.35
Campestanol	$C_{28}H_{50}O$	402.39	1	1	8.25	0.02
Campesterol	$C_{28}H_{48}O$	400.37	1	1	7.87	0.59
Clerosterol	$C_{29}H_{48}O$	412.37	1	1	8.58	0.68
Delta-5-avenasterol	$C_{29}H_{48}O$	412.37	1	1	7.82	0.85
Delta-7-avenasterol	$C_{29}H_{48}O$	412.37	1	1	7.95	0.25
Delta-tocopherol	$C_{27}H_{46}O_2$	402.35	2	1	9.20	0.33
D-galactose	$C_6H_{12}O_6$	180.06	6	5	-3.02	-0.12
Dl-alanine-15n	$C_3H_7NO_2$	89.05	3	3	-2.64	-0.96
Dl-arginine	$C_6H_{14}N_4O_2$	174.11	4	7	-3.93	-0.16
D-xylose	$C_5H_{10}O_5$	150.05	5	4	-2.93	-1.37
Gamma-tocopherol	$C_{28}H_{48}O_2$	416.37	2	1	9.48	0.48
Indole-3-acetic-acid	$C_{10}H_9NO_2$	175.06	2	2	1.62	0.50
Indoleacetonitrile	$C_{10}H_8N_2$	156.07	1	1	1.86	-2.06
Kaempferol	$C_{15}H_{10}O_6$	286.05	6	4	1.61	0.11
L-rhamnose	$C_6H_{12}O_5$	164.07	5	4	-2.30	-1.05
Maltotriose	$C_{18}H_{32}O_{16}$	504.17	16	11	-5.06	0.11
Phytosterols	$C_{29}H_{50}O$	414.39	1	1	8.45	0.78
Quercetin	$C_{15}H_{10}O_7$	302.04	7	5	1.19	0.52
Stigmastanol	$C_{29}H_{52}O$	416.40	1	1	8.83	0.22
Vanillin	$C_8H_8O_3$	152.05	3	1	0.96	-1.24
*Diclofenac	$C_{14}H_{11}Cl_2NO_2$	295.02	2	2	4.52	0.59

NHBA- Number of hydrogen bond acceptors, NHBD- Number of hydrogen bond donors, DLS- Drug-likeness score

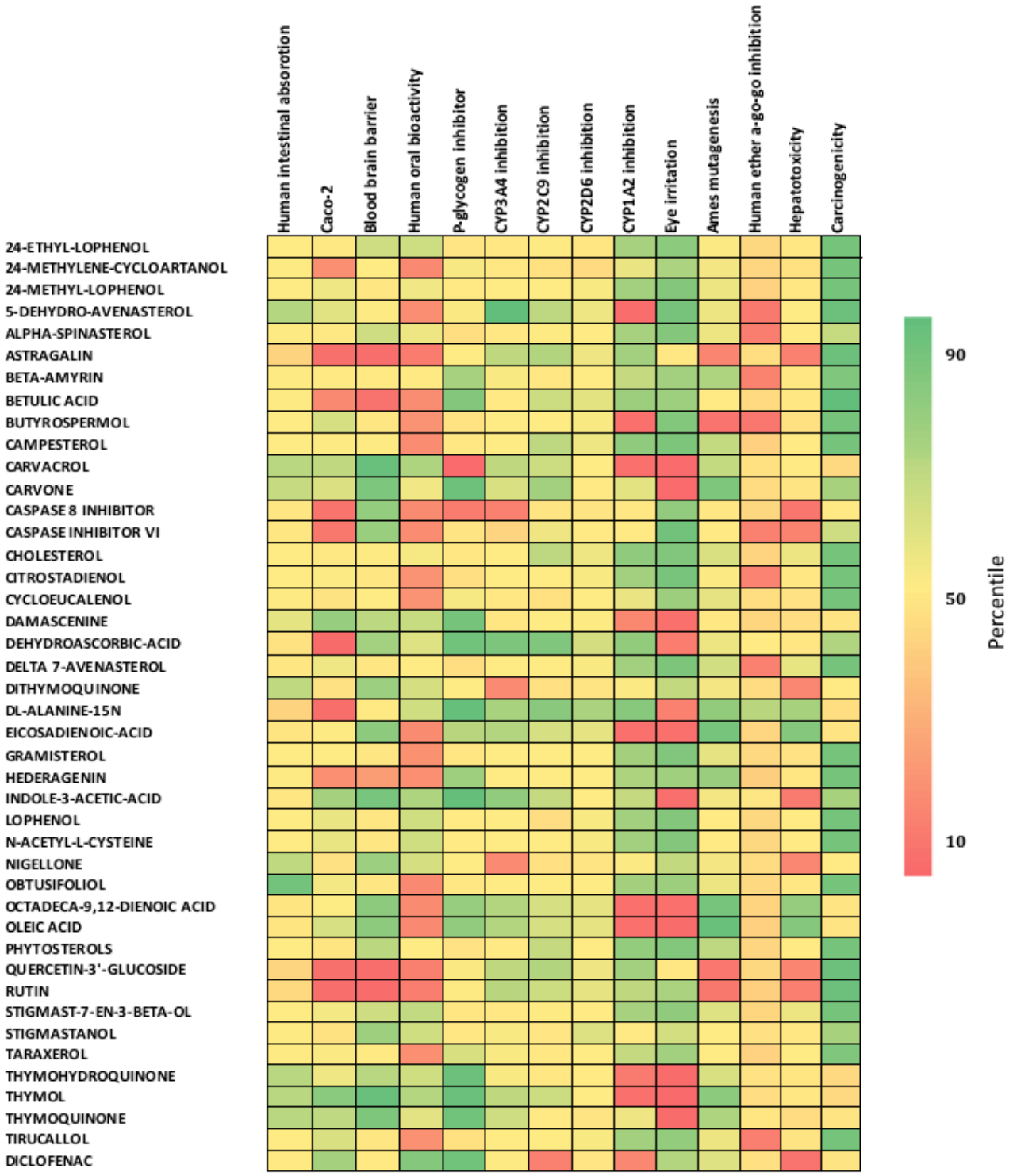

Figure 1 Heat map of ADMET profile of phytoconstituents of *Nigella sativa*

Green, yellow and red boxes indicate good, average and bad phytoconstituents for a particular parameter.

24-ethyl-lophenol, 24-methyl-lophenol, cholesterol, lophenol, N-acetyl-4-cysteine, phytosterols, stigmat-7-en-beta-ol and stigmastanol had perfect positive outcomes.

All the phytoconstituents from *M. oleifera* apart from D-galactose, DL-arginine, D-xylose, L-rhamnose and Maltotriose are predicted to have positive human intestinal absorption scores. All the phytoconstituents apart from 4-hydroxymellein, Caffeic acid, Kaempferol and Quercetin are blood-brain barrier permeants, eighteen phytoconstituents have positive bioavailability scores and all the compounds apart from 28-isoavenasterol acetate, Beta-sitosterone, Caffeic acid and Delta-5-avenasterol are predicted to be non-inhibitors of P-glycogen. Kaempferol and Quercetin are predicted to be inhibitors of CYP3A4, Benzyl-amine, Indoleacetonitrile and Kaempferol are predicted to be inhibitors of CYP2C9, Indoleacetonitrile is predicted to be an inhibitor of CYP2D6, 4-

hydroxymellein, Benzyl-amine, Indoleacetonitrile, Kaempferol and Quercetin are predicted to be inhibitors of CYP1A2. Nine phytoconstituents are predicted to cause eye irritation. 4-hydroxymellein, DL-arginine, D-xylose, Kaemferol and Quercetin are predicted to be mutagenic, eight phytoconstituents are predicted to be inhibitors of human ether a-go-go, Indole-3-acetic acid, Indoleacetonitrile, Kaempferol and Quercetin showed a tendency towards hepatotoxicity and Benzyl-amine showed tendency towards carcinogenicity.

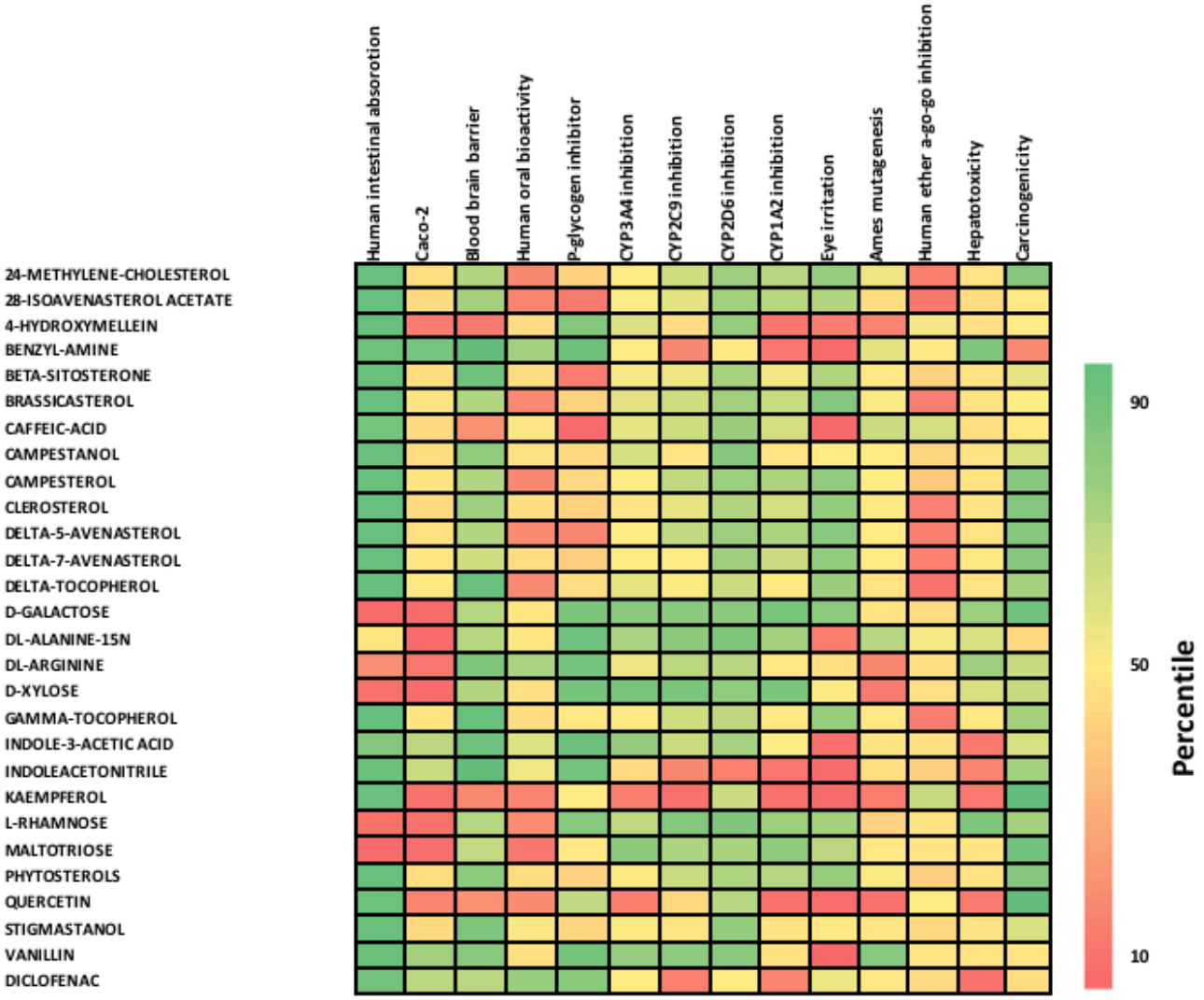

Figure 2 Heat map of ADMET profile of phytoconstituents of *Moringa oleifera*

Green, yellow and red boxes indicate good, average and bad phytoconstituents for a particular parameter.
Campestanol and stigmastanol had perfect positive outcomes.

Enrichment/network analysis

Gene set enrichment analysis identified thirty-three (33) modulated inflammatory pathways. The predicted pathways in inflammation having the highest count of the gene set were MAPK signaling pathway and cytomegalovirus infection with 18 proteins each (Table 5)

Table 5 Gene set Enrichment analysis of modulated inflammatory pathways

ID	Pathways	Count in Gene Set	Gene code
hsa04932	Non-alcoholic fatty liver disease	15	CASP7, NDUFA4, CASP3, PRKAB1, CXCL8, RXRA, CASP8, GSK3B, IL6, AKT1, TNF, PPARA, NFKB1, ERN1, NR1H3

hsa05310	Asthma	1	TNF
hsa04064	NF -kappa B signaling pathway	9	PTGS2, CXCL8, NFKBIA, BIRC2, TNF, MALT1, NFKB1, LCK, CSNK2A1
hsa05321	Inflammatory bowel disease	6	NFKB1, TNF, RORC, RORA, IL2, IL6
hsa05323	Rheumatoid arthritis	7	CTSK, CTSL, CXCL8, IL6, TNF, VEGFA, MMP1
hsa05412	Arrhythmogenic right ventricular cardiomyopathy	4	ITGA2B, ITGB3, CACNA1C, ATP2A1
hsa04062	Chemokine signaling pathway	7	CXCL8, NFKBIA, GSK3B, AKT1, CXCR1, NFKB1, PIK3CG
hsa04145	Phagosome	3	MPO, ITGB3, CTSS, CTSL
hsa04514	Cell adhesion molecules	1	PTPRC
hsa04659	Th17 cell differentiation	10	IL6, NFKBIA, RORC, RXRA, RORA, AHR, IL2, NFKB1, HSP90AA1, LCK
hsa04668	TNF signaling pathway	11	CASP7, CASP3, PTGS2, NFKBIA, BIRC2, CASP8, TNF, MMP9, NFKB1, IL6, AKT1
hsa04670	Leukocyte transendothelial migration	3	PRKCA, MMP2, MMP9
hsa04931	Insulin resistance	13	RPS6KA3, PRKAB1, NFKBIA, NOS3, GSK3B, IL6, AKT1, TNF, PPARA, NFKB1, PTPN1, NR1H2, NR1H3
hsa05322	Systemic lupus erythematosus	4	GRIN2B, ELANE, TNF, C5
hsa05416	Viral myocarditis	5	ABL1, ABL2, CASP3, CASP8, CASP9
hsa04614	Renin-angiotensin system	3	CMA, REN, ACE
hsa04933	AGE-RAGE signaling pathway in diabetic complications	12	NOS3, CASP3, PIM1, PRKCA, CXCL8, IL6, AKT1, TNF, VEGFA, NOX4, NFKB1, MMP2
hsa04010	MAPK signaling pathway	18	PGF, IGF1R, RPS6KA3, CASP3, AKT1, PRKCA, CACNA1C, EGFR, NTRK2, FLT3, MET, TNF, VEGFA, NFKB1, KIT, PTPN7, FGF2, FGF1
hsa05418	Fluid shear stress and atherosclerosis	12	ITGB3, NOS3, CTSL, ITGA2B, NFKB1, AKT1, GSTP1, TNF, VEGFA, MMP9, HSP90AA1, MMP2
hsa04066	HIF-1 signaling pathway	9	IGF1R, NOS3, PRKCA, EGFR, NOS2, IL6, AKT1, VEGFA, NFKB1
hsa04610	Complement and coagulation cascades	4	F2, F10, C5, F7
hsa04657	IL-17 signaling pathway	12	PTGS2 , CASP3, NFKBIA, CASP8, TNF, MMP9, NFKB1, CXCL8, GSK3B, MMP1, IL6, HSP90AA1
hsa04658	Th1 and Th2 cell differentiation	4	NFKB1, NFKBIA, IL2, LCK
hsa04664	Fc epsilon RI signaling pathway	4	PRKCA, AKT1, ALOX5, TNF
hsa05010	Alzheimer disease	17	CASP7, NDUFA4, ATP2A1, BACE1, PSEN1, CACNA1C, CASP8, CASP9, GRIN2B, TNF, CAPN2, CAPN1, CDK5, GRIN1, GSK3B, ERN1, CASP3
hsa05150	*Staphylococcus aureus* infection	1	C5
hsa05163	Human cytomegalovirus	18	PTGS2, ITGB3, CASP3, PTGER4, CXCL8, PRKCA,

	infection		NFKBIA, EGFR, CASP8, PTGER3, IL6, AKT1, TNF, VEGFA, GSK3B, CDK6, NFKB1, CASP9
hsa05166	Human T-cell leukemia virus 1 infection	9	NFKBIA, IL6, AKT1, CDK2, TNF, IL2, NFKB1, TERT, LCK
hsa05167	Kaposi sarcoma-associated herpesvirus infection	14	PTGS2, CASP3, CXCL8, NFKBIA, CASP8, CASP9, IL6, AKT1, VEGFA, GSK3B, CDK6, NFKB1, PIK3CG, FGF2
hsa05203	Viral carcinogenesis	16	HDAC1, HDAC3, HDAC2, HDAC5, CASP3, HDAC6, HDAC9, HDAC8, NFKBIA, CASP8, CDK1, CDK2, CDK6, NFKB1, HDAC10, HDAC4
hsa05206	MicroRNAs in cancer	17	HDAC1, PTGS2, ITGB3, CYP24A1, CYP1B1, CASP3, PIM1, PRKCA, EGFR, MET, VEGFA, CDK6, MMP9, ABL1, NFKB1, ABCC1, HDAC4
hsa05225	Hepatocellular carcinoma	10	IGF1R, AKT1, PRKCA, EGFR, GSK3B, MET, GSTP1, CDK6, TERT, TXNRD1
hsa05231	Choline metabolism in cancer	3	PRKCA, AKT1, EGFR

Protein-protein network

The protein-protein interaction (PPI) network is shown in Figure 3. RAC-alpha serine/threonine protein kinase (AKT1) and heat shock protein HSP 90-alpha (HSP90AA1) had the highest interactions, interacting with 31 proteins each at a 70% confidence level. The levels of AKT1, HSP90AA1 and TNF-α were e express.

Network pharmacology analysis

Seven hundred and ninety-seven (797) edges were identified in the component-target-pathway network in which five hundred and fourteen (514) were target-components interactions and two hundred and eighty-three (283) were target-pathway interactions (Figure 4). The constructed network included one hundred and ninety-six (197) nodes representing sixty-seven (67) phytoconstituents, ninety-eight (97) targets and thirty-three (33) pathways. Prothrobin scored the highest edge count; interaction was found with thirty-one (31) protein molecules. Similarly, the MAPK signaling pathway and human cytomegalovirus infection modulated the highest number of proteins (eighteen proteins apiece). Rutin, beta-sitosterone, astragalin, beta-amyrin, quercetin and 4-hydroxymellein are the most important nodes of the entire network.

Molecular docking analysis

The phytoconstituents of *N. sativa* and *M. oleifera* interacted with the selected inflammatory targets at different levels of binding affinity. Table 6 shows the binding affinities of different compounds selected based on the results from the network analysis and the different proteins selected. The binding energies of most of the compounds were lower than -5Kcal/mol. To further validate the results of network pharmacology, most of the phytoconstituents of *N. sativa* and *M. oleifera* were docked with the predicted targets in addition to interferon-gamma. The results showed that some of the compounds had lower binding affinities than the ones predicted by network pharmacology. However, most of the compounds predicted by network pharmacology interacted with more amino acid residues and formed more hydrogen bonds with the amino acid residues. Table 7 shows the binding affinities of most of the compounds from *N. sativa* and *M. oleifera.* Figures 5-15 show the three-dimensional (3D) and two-dimensional (2D) representations of the molecular interactions of the amino acid residues of the targets with the compounds predicted to have the lowest binding energies, with Figures 5-14A representing those predicted by network pharmacology and figures 5-14B representing those predicted after docking with most of the compounds.

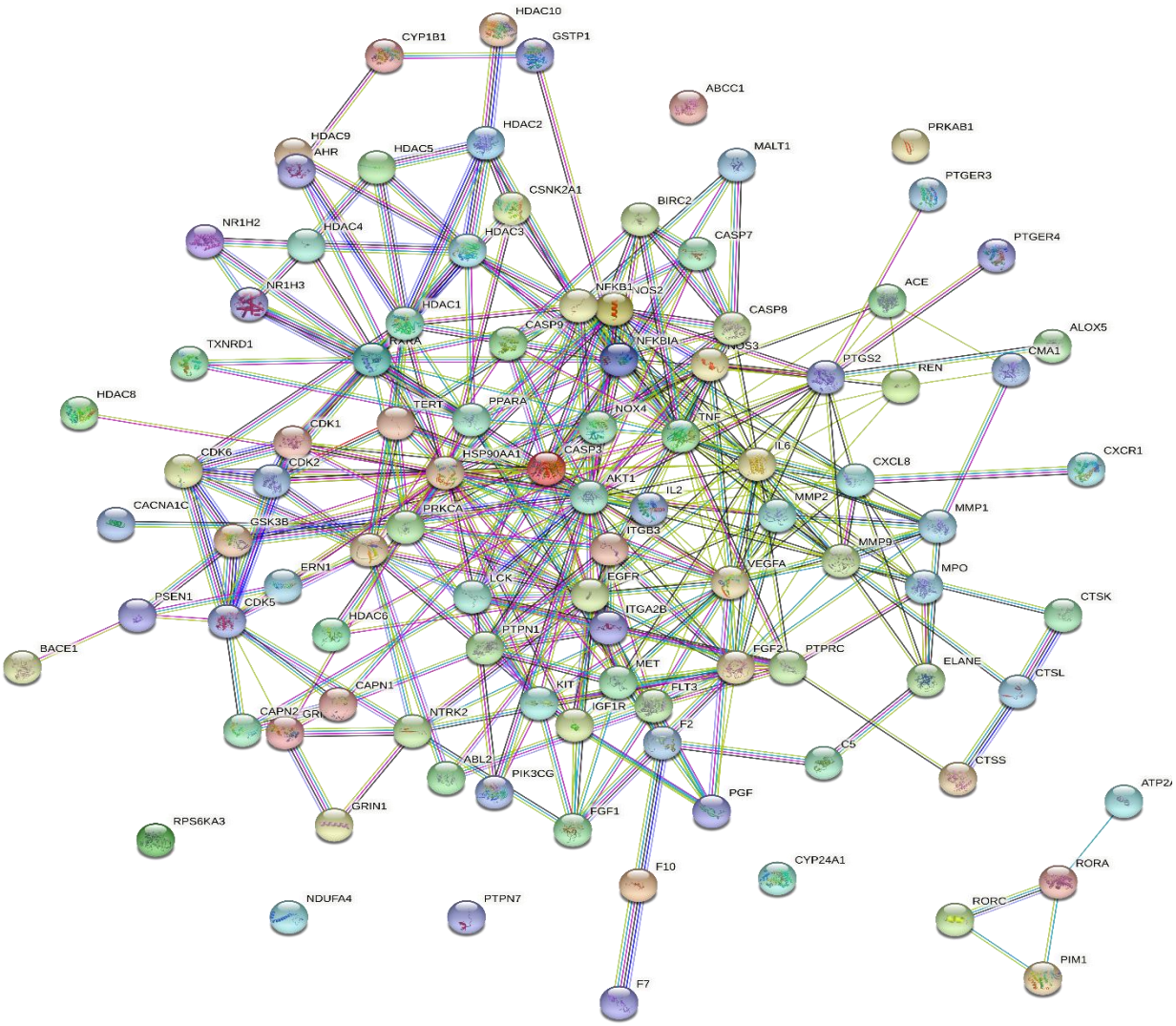

Figure 3 Protein-protein interaction of regulated proteins by the phytoconstituents from *N. sativa* and *M. oleifera.*

Each node (circle) represents a protein and each line refers to an interaction. The thickness of the line reflects the strength of the protein-protein interaction. Circles without lines linking them to other circles indicate that the protein interacted with no other protein.

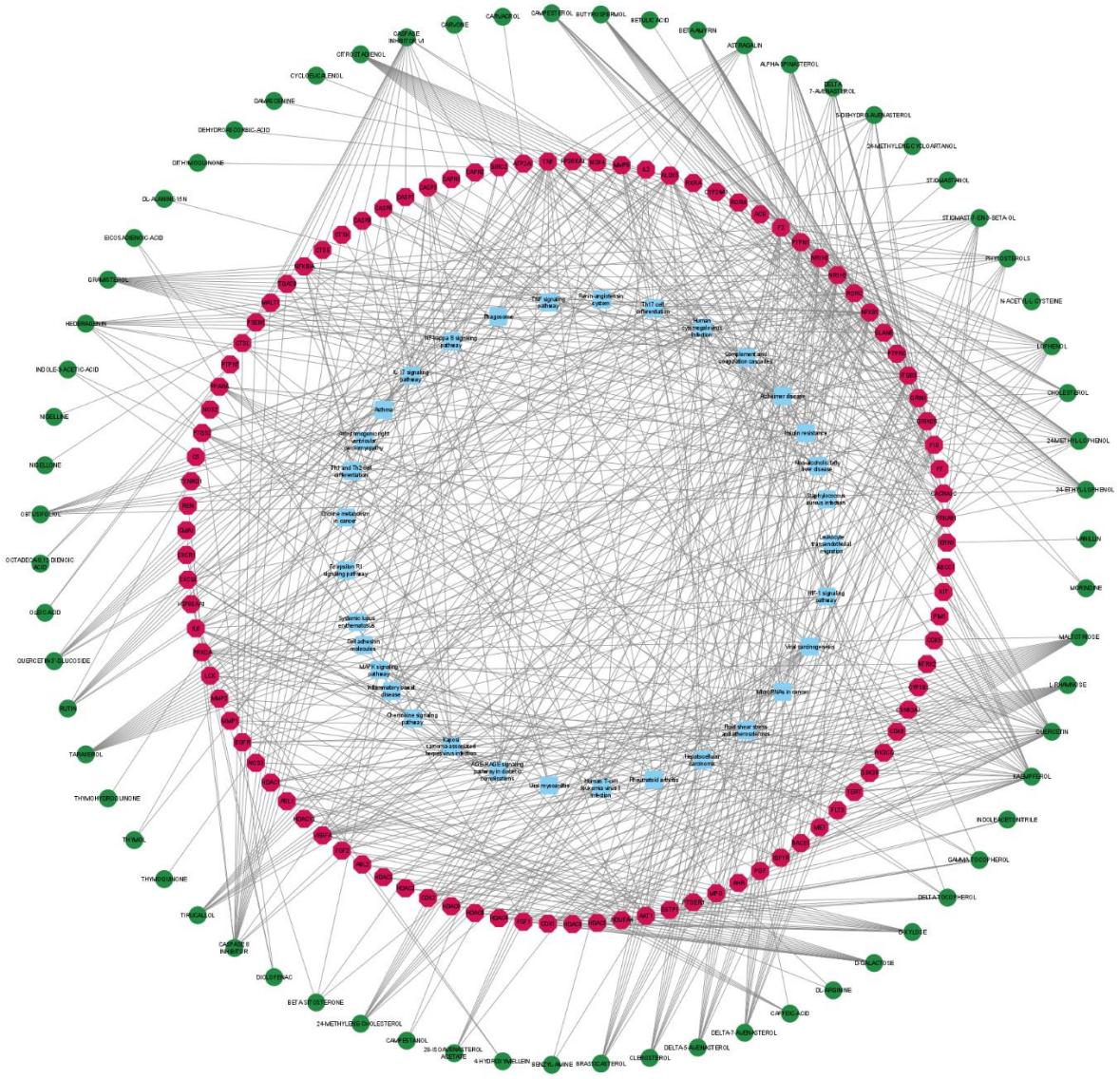

Figure 4 Components–targets–pathways network of phytoconstituents of *N. sativa* and *M. olifera*
Green, pink and blue colours indicate the phytoconstituents, targets and pathways respectively. The lines (edges) represent the interactions.

Table 6 Binding affinities of compounds of *N. sativa* and *M. oleifera* against the selected targets

Phytoconstituents	PubChem CID	ΔG Energy (Kcal/mol)										
		NR1H3	F2	AKT1	HSP90 AA1	IL2	NFKB1	PTGS 2	ALOX5	TNF	IL6	IFN-γ
24-methylene cycloartenol	94204	-11.2	-8.4	-5.7	-8.1	-5.3	-6.4	-7.4	-8.1	-6.3	-6.4	-8.9
24-methylene-cholesterol	92113	-8.9	-7.5	-6.7	-8.6	-5.5	-6.7	-7.6	-8.2	-6.4	-6.1	-8.3
28-isoavenasterol acetate	91746804	-8.1	-7.5	-5.6	-7.2	-5.3	-5.9	-7.2	-8.1	-5.2	-6.3	-8.4
4-hydroxymellein	169539	-7.6	-5.7	-4.8	-6.7	-4.5	-5.7	-6.8	-7.4	-4.9	-5.5	-5.8
5-dehydro-avenasterol	44263331	-8.9	-8.2	-6.6	-8.7	-5.8	-7.1	-7.9	-9.0	-6.6	-5.9	-8.8
Alpha-spinasterol	5281331	-8.8	-8.3	-6.1	-8.6	-5.8	-6.8	-9.2	-9.6	-6.2	-7.0	-8.9
Astragalin	5282102	-9.1	-7.8	-5.4	-8.8	-5.4	-7.0	-8.4	-7.9	-5.7	-6.4	-6.8
Benzyl-amine	7504	-5.8	-4.6	-3.7	-4.9	-3.1	-4.3	-5.2	-5.2	-3.8	-3.5	-4.3

Beta-amyrin	73145	-9.7	-8.7	-6.5	-7.6	-6.5	-7.8	-9.2	-10.0	-6.8	-6.5	-10.7
Beta-sitosterone	9801811	-8.1	-7.6	-6.7	-8.4	-5.8	-6.1	-7.3	-8.6	-6.1	-6.2	-8.0
Brassicasterol	5281327	-12.0	-7.9	-6.7	-7.7	-5.5	-6.6	-9.0	-9.2	-6.7	-6.1	-8.6
Butulic acid	64971	-9.2	-7.4	-5.9	-6.6	-5.8	-6.7	-8.1	-9.4	-6.6	-6.3	-8.4
Butyrospermol	12302182	-10.0	-8.6	-6.0	-8.8	-5.7	-6.9	-7.5	-9.1	-5.5	-6.9	-9.8
Caffeic acid	689043	-7.1	-6.1	-4.2	-5.9	-4.7	-5.1	-6.9	-6.8	-4.7	-5.1	-6.1
Campestanol	119394	-11.2	-7.3	-6.4	-8.3	-5.3	-6.5	-7.5	-8.4	-6.4	-6.1	-8.3
Campesterol	173183	-10.0	-8.0	-6.5	-8.5	-5.4	-6.6	-8.8	-8.4	-6.5	-5.8	-9.1
Carcacol	10364	-7.2	-5.5	-4.3	-5.9	-4.4	-4.6	-6.6	-7.0	-4.2	-4.4	-5.7
Carvone	7439	-6.9	-5.2	-4.1	-5.8	-4.2	-4.5	-6.6	-6.5	-4.4	-4.3	-5.4
Cholesterol	5997	-11.6	-7.8	-6.3	-8.1	-5.4	-6.4	-8.6	-7.9	-6.0	-5.8	-8.2
Citrostadienol	9548595	-11.6	-8.0	-5.8	-8.9	-5.8	-6.3	-9.3	-8.5	-7.1	-6.7	-9.5
Clerosterol	5283638	-11.5	-7.4	-6.3	-8.3	-5.6	-6.2	-7.2	-8.9	-6.0	-5.8	-8.2
Cycloeucalenol	101690	-8.2	-8.2	-5.6	-8.3	-5.9	-6.8	-9.2	-8.6	-6.5	-6.7	-8.6
Damascenine	21368	-6.7	-5.2	-3.9	-5.5	-3.8	-4.6	-6.3	-6.3	-4.2	-4.3	-5.0
Dehydroascorbic acid	440667	-5.5	-5.8	-4.3	-6.1	-4.1	-5.0	-6.5	-6.4	-4.9	-4.9	-4.6
Delta-5-avenasterol	5281326	-9.6	-7.5	-6.7	-8.1	-5.4	-6.4	-7.6	-8.2	-6.9	-6.0	-9.6
Delta-7-avenasterol	12795733	-11.0	-8.5	-6.1	-8.8	-5.5	-7.0	-8.4	-8.9	-6.6	-6.6	-8.9
Delta-tocopherol	92094	-8.9	-6.0	-4.3	-7.0	-4.5	-4.9	-7.0	-7.8	-4.3	-5.3	-7.7
D-galactose	6036	-5.8	-4.8	-4.4	-5.6	-3.8	-4.7	-6.2	-6.1	-4.4	-4.7	-5.1
Dithymoquinone	398941	-7.9	-7.3	-5.3	-6.7	-5.1	-6.3	-7.5	-8.4	-5.7	-6.0	-7.4
D-xylose	135191	-5.3	-5.9	-4.3	-5.0	-3.5	-4.5	-5.7	-5.3	-4.1	-3.9	-4.6
Gamma-tocopherol	92729	-7.6	-6.3	-.4.3	-6.8	-4.6	-5.2	-7.6	-6.8	-4.8	-5.6	-8.3
Gramisterol	5283640	-8.0	-7.4	-6.3	-8.5	-5.5	-6.3	-8.4	-8.6	-6.6	-6.6	-8.7
Hederagenin	73299	-8.8	-7.7	-6.1	-7.3	-6.2	-7.2	-8.4	-9.1	-6.2	-6.3	-9.8
Indole-3-acetic acid	802	-7.4	-5.8	-4.5	-6.7	-4.5	-4.9	-6.8	-7.0	-4.8	-5.0	-5.7
Indoleacetonitrile	351795	-7.1	-5.7	-4.3	-6.4	-3.9	-5.1	-6.4	-6.8	-4.6	-4.7	-5.9
Kaempferol	5280863	-8.9	-7.4	-5.7	-7.4	-5.5	-6.4	-9.3	-8.0	-5.8	-6.0	-6.7
Lophenol	160482	-11.3	-7.7	-5.9	-8.2	-5.2	-6.4	-7.0	-8.5	-6.1	-6.4	-8.7
L-rhamnose	25310	-5.4	-4.9	-4.3	-5.4	-3.7	-4.6	-5.9	-5.7	-4.0	-4.5	-4.2
Maltotriose	439586	-7.2	-7.0	-4.8	-7.7	-5.1	-6.3	-6.7	-7.6	-5.1	-5.4	-5.6
N-acetyl-L-cysteine	12035	-5.3	-4.5	-3.4	-5.0	-3.4	-4.0	-4.9	-5.0	-3.9	-3.8	-3.9
Obtusifoliol	65252	-8.1	-7.9	-5.9	-8.2	-5.3	-6.9	-8.1	-8.9	-6.3	-6.6	-9.2
Octadeca-9,12-dienoic acid	3931	-7.2	-5.1	-4.4	-5.6	-3.3	-4.7	-5.8	-5.8	-3.9	-4.6	-5.8
Oleic acid	445639	-6.9	-5.3	-3.6	-5.2	-3.8	-4.0	-5.6	-5.8	-3.9	-4.2	-5.6
Phytosterols	12303662	-8.3	-8.1	-6.4	-8.6	-5.3	-6.1	-7.2	-8.8	-6.2	-5.6	-8.1
Quercetin	5280343	-9.1	-8.1	-5.5	-7.5	-5.6	-6.7	-9.4	-8.3	-5.7	-6.4	-6.6
Quercetin-3′-glucoside	25203368	-8.8	-8.5	-6.1	-8.5	-5.4	-6.6	-8.9	-7.9	-6.1	-6.7	-6.8
Rutin	5280805	-9.3	-8.3	-6.5	-7.7	-6.2	-7.5	-10.0	-8.6	-6.8	-6.6	-7.7
Stigmast-7-en-3-beta-ol	441837	-11.1	-8.2	-5.7	-7.7	-5.7	-6.7	-7.4	-8.4	-6.3	-6.7	-8.6
Stigmastanol	241572	-11.1	-7.6	-6.3	-8.4	-5.2	-6.1	-7.3	-8.3	-6.1	-6.1	-8.0
Taraxerol	92097	-10.0	-8.1	-7.2	-7.3	-6.8	-7.6	-9.1	-9.9	-6.5	-6.7	-10.1
Thymohydroquinone	95779	-6.7	-5.5	-4.1	-6.2	-4.0	-4.7	-6.3	-7.1	-4.3	-4.8	-5.4
Thymol	6989	-6.7	-5.4	-4.1	-5.8	-4.0	-4.8	-6.0	-7.1	-4.0	-4.7	-5.7
Thymoquinone	10281	-7.0	-5.5	-4.0	-6.4	-3.9	-4.6	-6.7	-7.3	-4.3	-4.7	-5.3
Tirucallol	101257	-9.2	-7.2	-7.1	-7.8	-5.4	-6.7	-8.6	-9.5	-6.0	-7.0	-9.5

Vanillin	1183	-6.4	-5.4	-3.9	-5.6	-3.9	-4.6	-6.1	-6.1	-4.2	-4.1	-4.5
*Diclofenac	3033	-7.9	-6.7	-5.2	-7.9	-4.7	-5.7	-7.7	-7.1	-5.0	-5.1	-6.1

Table 7 Binding affinities of the compounds against the selected targets based on network pharmacology

Compounds	PubChem CID	ΔG Energy (Kcal/mol)									
		NR1H3	F2	AKT1	HSP90AA1	IL2	NFKB1	PTGS2	ALOX5	TNF	IL6
24-methylene cycloartanol	94204	-11.3	-	-	-	-	-	-	-	-	-
24-methylene-cholesterol	92113	-6.8	-8.5	-	-	-	-	-	-	-	-
28-isoavenasterol acetate	91746804	-6.9	-	-	-	-	-	-	-	-	-
4-hydroxymellein	169539	-	-	-	-	-	-	-	-	-	-5.1
5-dehydro-avenasterol	44263331	-7.0	-8.0	-	-	-	-	-	-	-	-
Alpha-spinasterol	5281331	-7.0	-7.8	-	-	-	-	-	-	-	-
Astragalin	5282102	-	-8.2	-	-	-5.5	-	-	-8.0	-5.7	-
Benzyl-amine	7504	-	-4.5	-	-	-	-	-	-	-	-
Beta-amyrin	73145	-7.7	-8.7	-	-	-	-7.5	-	-	-	-
Beta-sitosterone	9801811	-6.7	-	-	-7.1	-	-	-	-	-	-
Brassicasterol	5281327	-7.2	-7.7	-	-	-	-	-	-	-	-
Butyrospermol	12302182	-10.6	-7.3	-	-	-	-7.0	-	-	-	-
Campestanol	119394	-11.2	-	-	-	-	-	-	-	-	-
Campesterol	173183	-12.3	-8.2	-	-	-	-	-	-	-	-
Cholesterol	5997	-11.7	-7.9	-	-	-	-	-	-	-	-
Citrostadienol	9548595	-7.6	-8.1	-	-	-	-6.6	-	-	-	-
Clerosterol	5283638	-6.8	-7.4	-	-	-	-	-	-	-	-
Cycloeucalenol	101690	-10.8	-	-	-	-	-	-	-	-	-
Damascenine	21368	-	-	-	-	-	-	-	-5.4	-	-
Dehydroascorbic acid	440667	-	-	-	-	-	-	-	-5.9	-	-
Delta-5-avenasterol	5281326	-13.0	-7.4							-	
Delta-7-avenasterol	12795733	-11.3	-8.5	-	-	-	-	-	-	-	-
Delta-tocopherol	92094	-	-	-4.3	-	-	-	-7.7	-7.2	-	-
D-galactose	6036	-	-4.9	-	-	-	-	-	-	-	-
D-xylose	135191	-	-6.0	-	-	-	-	-	-	-	-
Gamma-tocopherol	92729	-8.1	-	-4.5	-	-	-	-7.5	-6.3	-	-
Gramisterol	5283640	-11.5	-7.9	-	-	-	-6.3	-	-	-	-
Hederagenin	73299	-7.7	-	-	-	-	-7.1	-8.7	-	-	-
Indole-3-acetic acid	802	-	-	-	-	-	-	-6.7	-	-	-
Kaempferol	5280863	-	-7.2	-	-	-	-	-7.7	-8.2	-	-
Lophenol	160482	-11.7	-7.6	-	-	-	-6.4	-	-	-	-
L-rhamnose	25310	-	-4.9	-	-	-	-	-	-	-	-
Maltotriose	439586	-	-7.0	-	-	-	-	-	-	-	-
Obtusifoliol	65252	-10.7	-7.8	-	-	-	-	-	-	-	-
Phytosterols	12303662	-6.7	-8.0	-	-	-	-	-	-	-	-
Quercetin	5280343	-	-7.2	-	-	-	-	-9.5	-8.3	-	-
Quercetin-3′-glucoside	25203368	-	-7.6	-	-	-5.4	-	-	-7.6	-5.8	-
Rutin	5280805	-	-8.7	-	-	-6.2	-	-	-8.6	-6.9	-
Stigmast-7-en-3-beta-ol	441837	-7.2	-8.2	-	-	-	-	-	-	-	-
Stigmastanol	241572	-6.9	-	-	-	-	-	-	-	-	-
Taraxerol	92097	-	-8.1	-	-	-	-7.3	-	-	-	-
Thymol	6989	-	-	-	-	-	-	-	-7.1	-	-

Thymoquinone	10281	-	-	-	-	-	-	-	-6.1	-	-
Tirucallol	101257	-7.5	-7.8	-	-	-	-	-	-	-	-
*Diclofenac	3033	-	-	-	-	-	-	-7.7	-	-	-

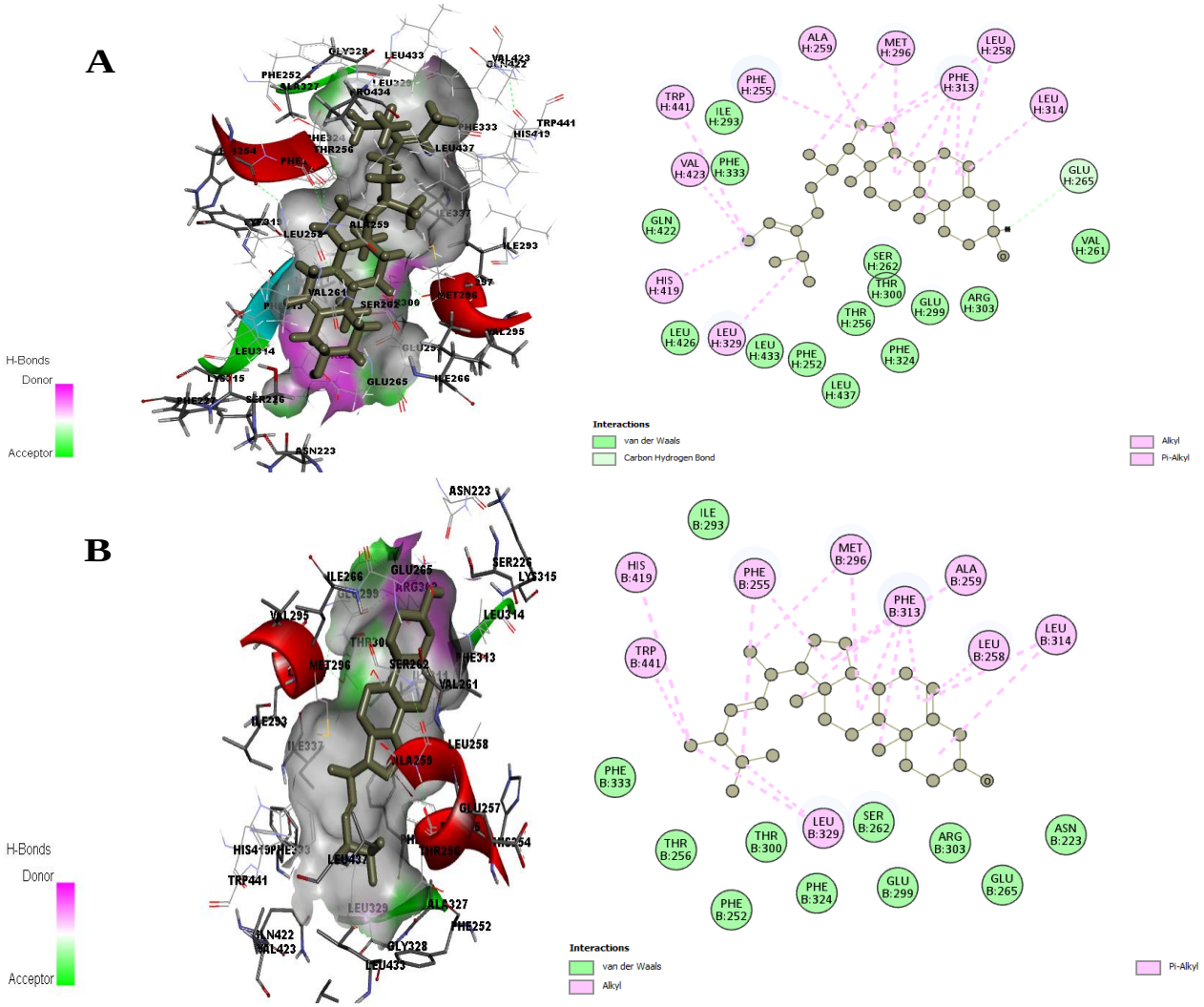

Figure 5 Molecular interactions of amino-acid residues of NR1H3 with A. Delta-5-avenasterol and B. Brassicasterol showing the 2D (right) and 3D (left) views

A. Delta-5-avenasterol interacted with different amino-acid residues in the binding site of NR1H3 forming pi-sigma, alkyl, pi-alkyl bonds as well as van der Waals forces. B. Brassicasterol reacts with different amino acid residues at the binding site of NR1H3 forming alkyl and pi-alkyl bonds and van der Waals forces with the protein.

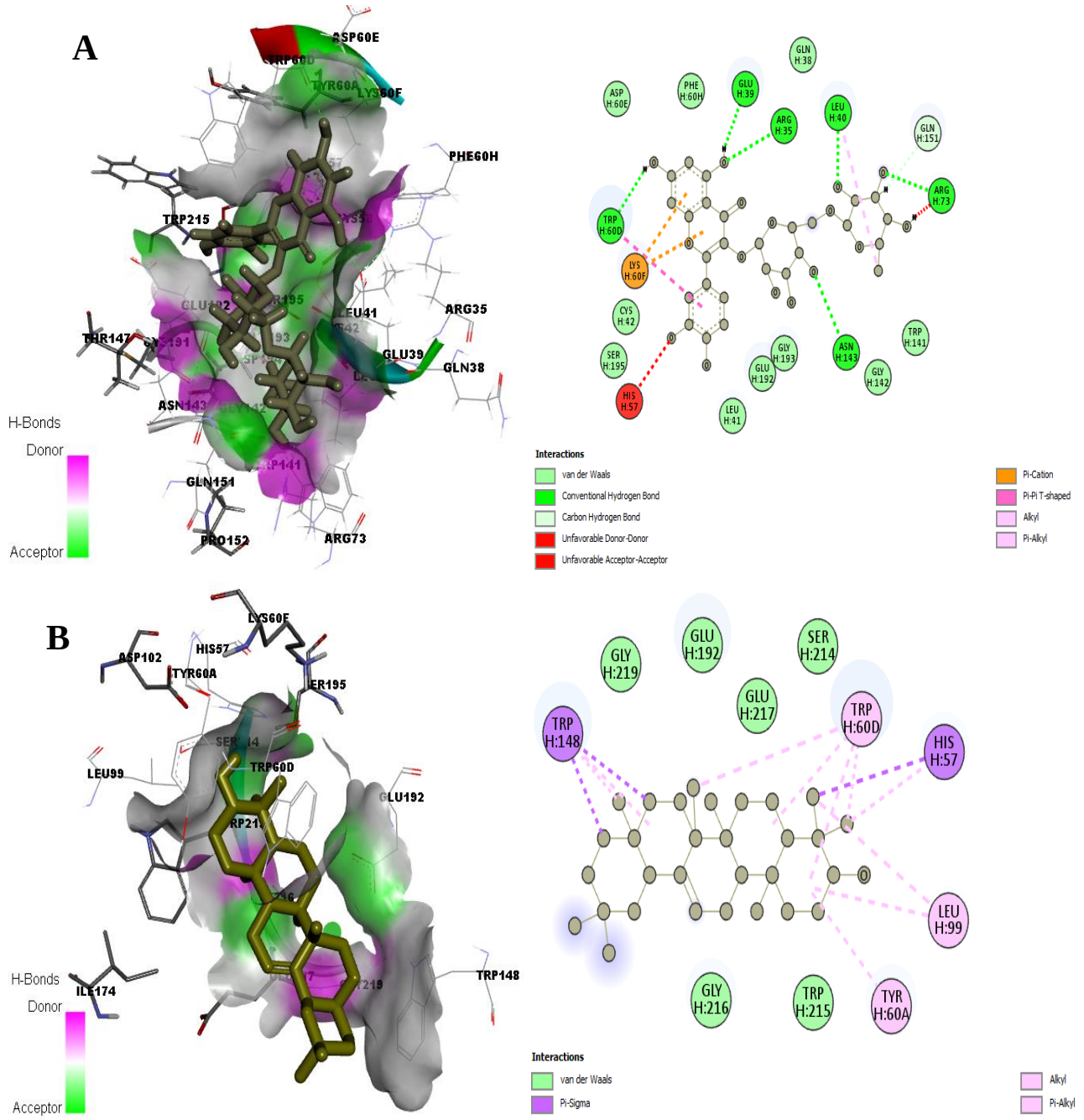

Figure 6 Molecular interactions of amino-acid residues of F2 with A. Rutin and B. Beta-amyrin showing the 2D (right) and 3D (left) views

A. Rutin interacted with different amino acid residues present in the binding site of F2 forming different kinds of bonds. Rutin formed hydrogen bonds with ARG35, GLU39, LEU40, TRP60D, ARG73 and ASN143. B. Beta-amyrin reacts with different amino acid residues at the binding site of F2 forming alkyl, pi-alkyl, pi-sigma bonds and van der Waals forces with the protein.

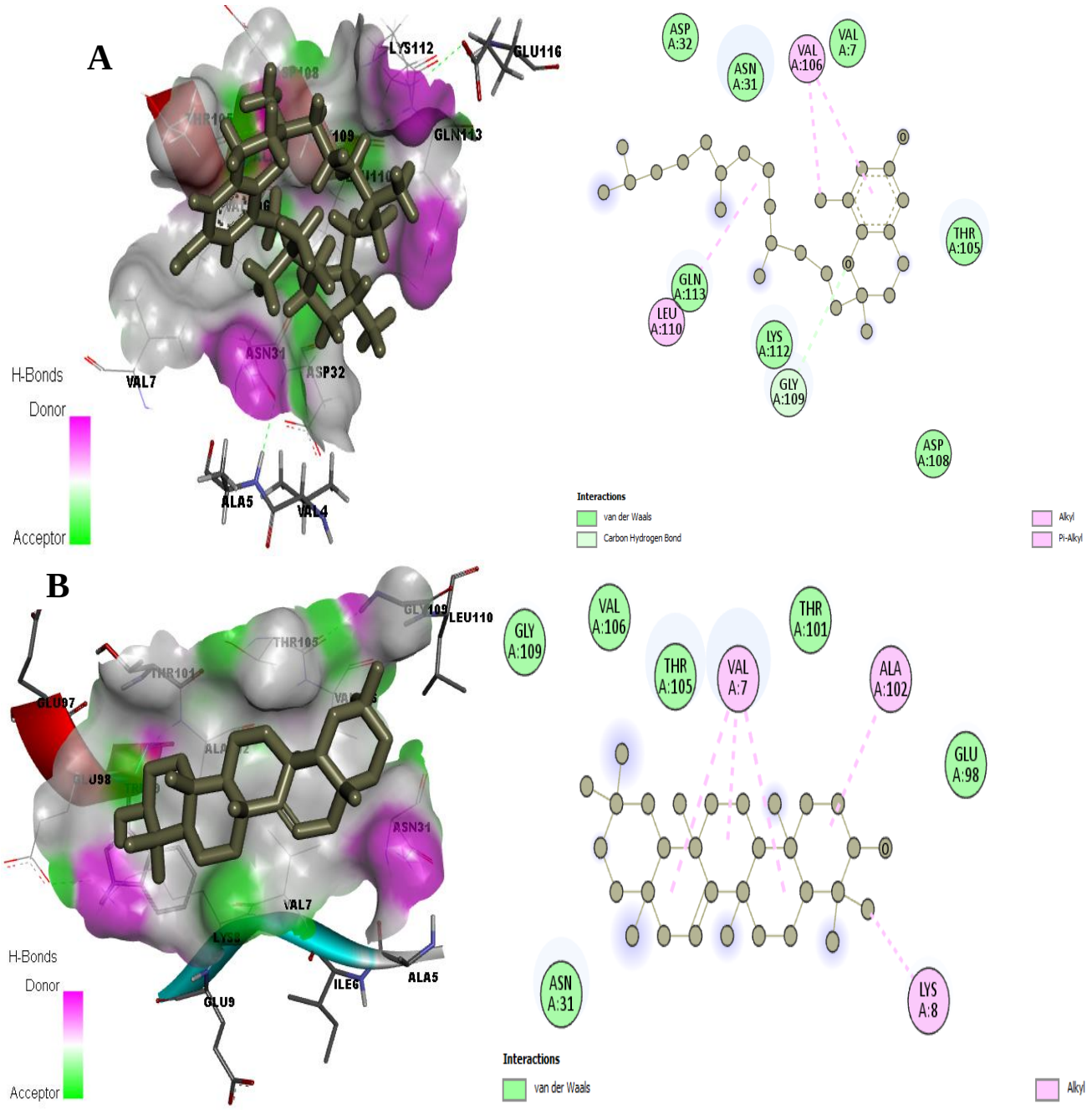

Figure 7 Molecular interactions of amino-acid residues of AKT1 with A. Delta-tocopherol and B. Taraxerol showing the 2D (right) and 3D (left) views

A. Delta-tocopherol interacted with VAL7, ASN31, ASP32, THR105, VAL106, GLY109, LEU110, LYS112 and GLN113 present in the binding site of AKT1 forming different kinds of bonds with the protein. B. Taraxerol reacts with different amino acid residues at the binding site of F2 forming alkyl bonds and van der Waals forces with the protein.

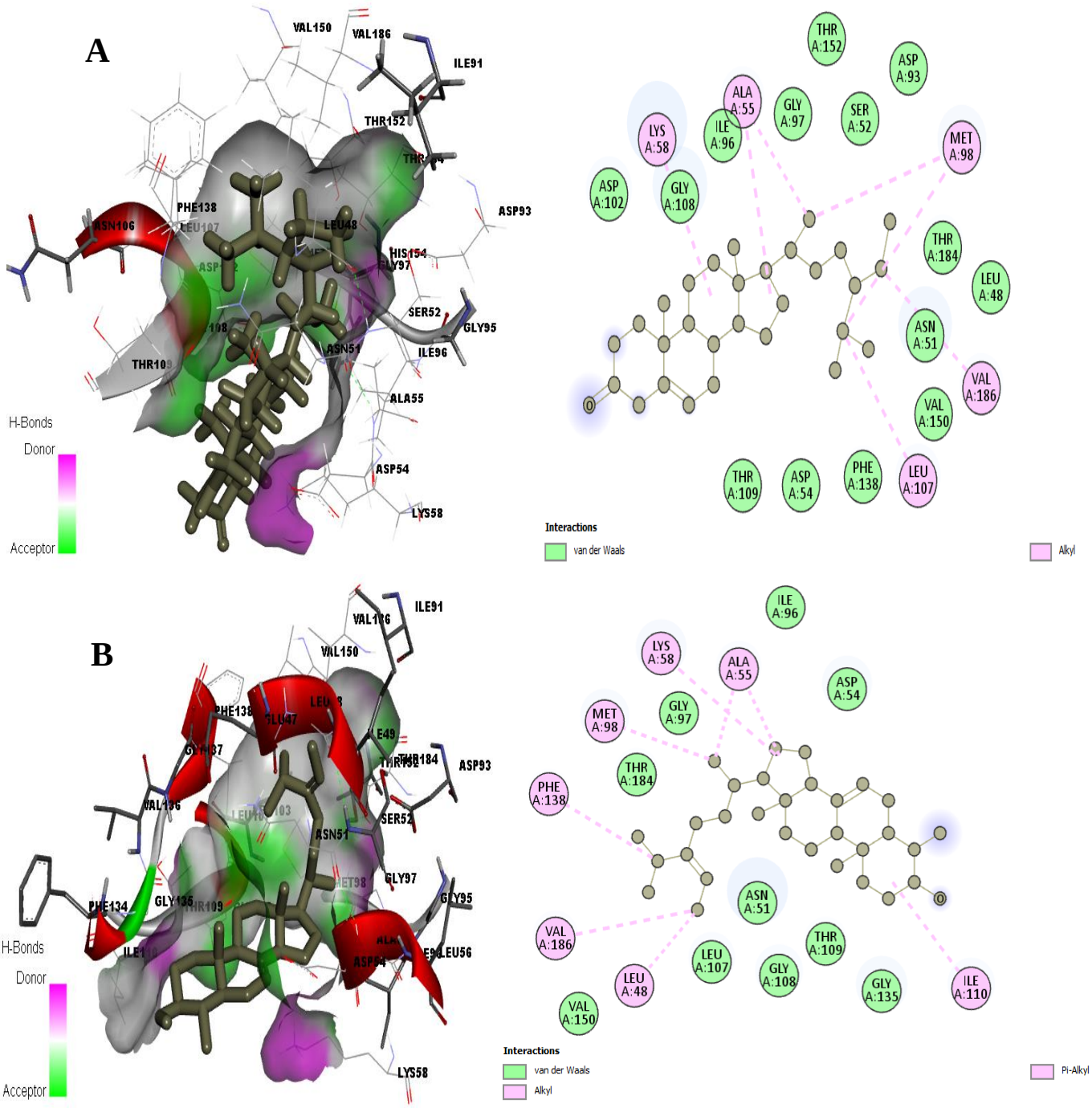

Figure 8 Molecular interactions of amino-acid residues of HSP90AA1 with A. Beta-sitosterone and B. Citrostadienol showing the 2D (right) and 3D (left) views

A. Beta-sitosterone interacted with different amino acid residues present in the binding site of HSP90AA1 forming alkyl bonds and van der Waals forces with the protein. B. Citrostadienol reacts with different amino acid residues at the binding site to HSP90AA1 forming alkyl and pi-alkyl bonds and van der Waals forces with the protein. alkyl bonds and van der Waals forces with the protein.

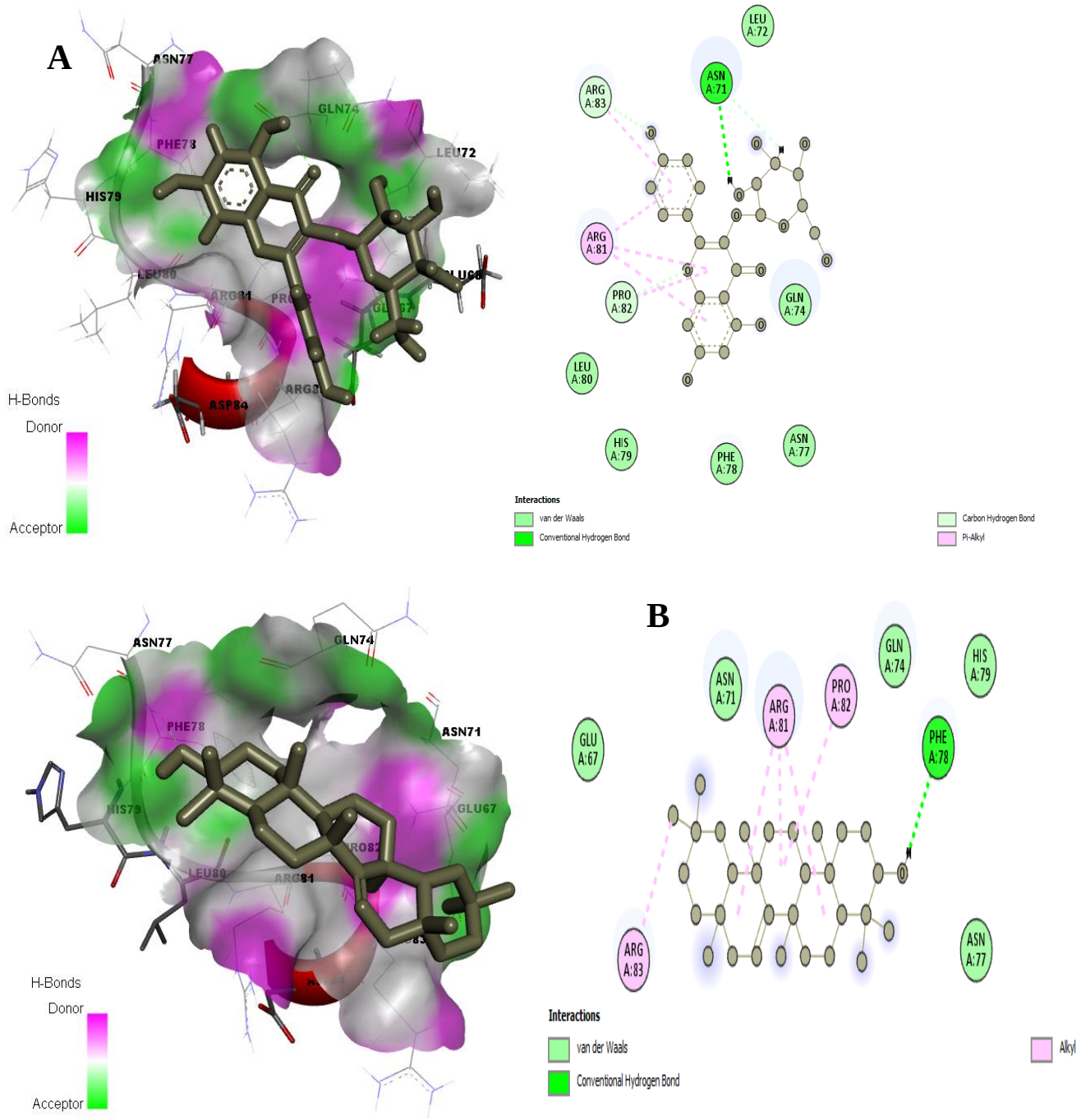

Figure 9 Molecular interactions of amino-acid residues of IL2 with A. Astragalin and B. Taraxerol showing the 2D (right) and 3D (left) views

A. Astragalin formed two hydrogen bonds at the target site of IL2, one of which is a conventional hydrogen bond with ASN71. Astragalin also formed a pi-alkyl bond with ARG81 and van der Waals forces with different amino acid residues. B. Taraxerol binds at the target site of IL-2 with one conventional hydrogen bond (PHE78), alkyl bonds with ARG81, PRO82 and ARG83 and five van der Waals forces (GLU67, ASN71, GLN74, ASN77 and HIS79).

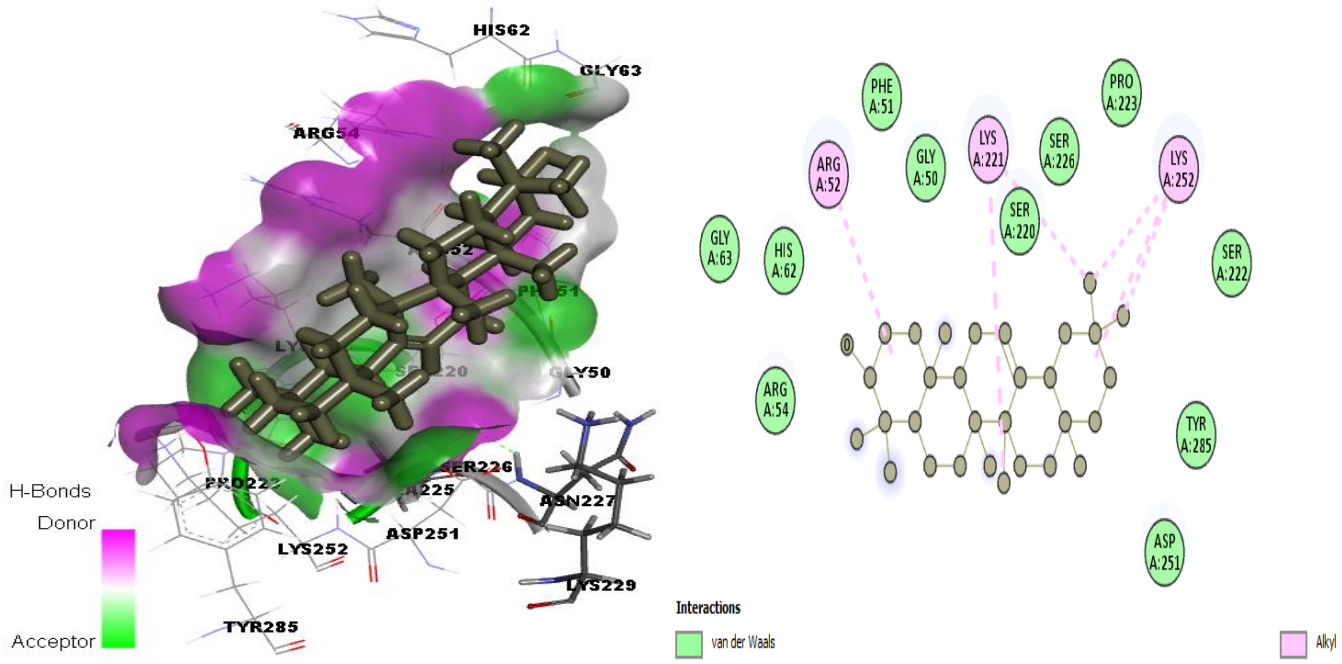

Figure 10 Molecular interactions of amino-acid residues of NFKB1 with beta-amyrin showing the 2D (right) and 3D (left) views Beta-amyrin reacts with different amino acid residues at the binding site of NFKB1 forming alkyl bonds and van der Waals forces with the protein.

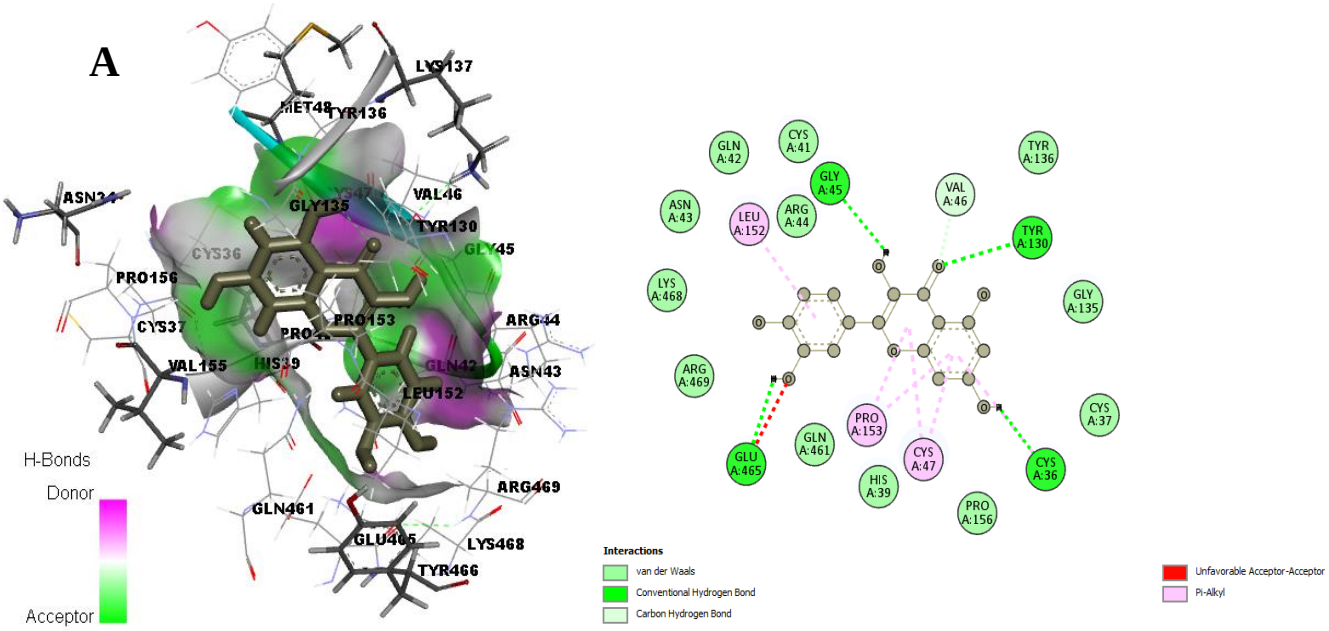

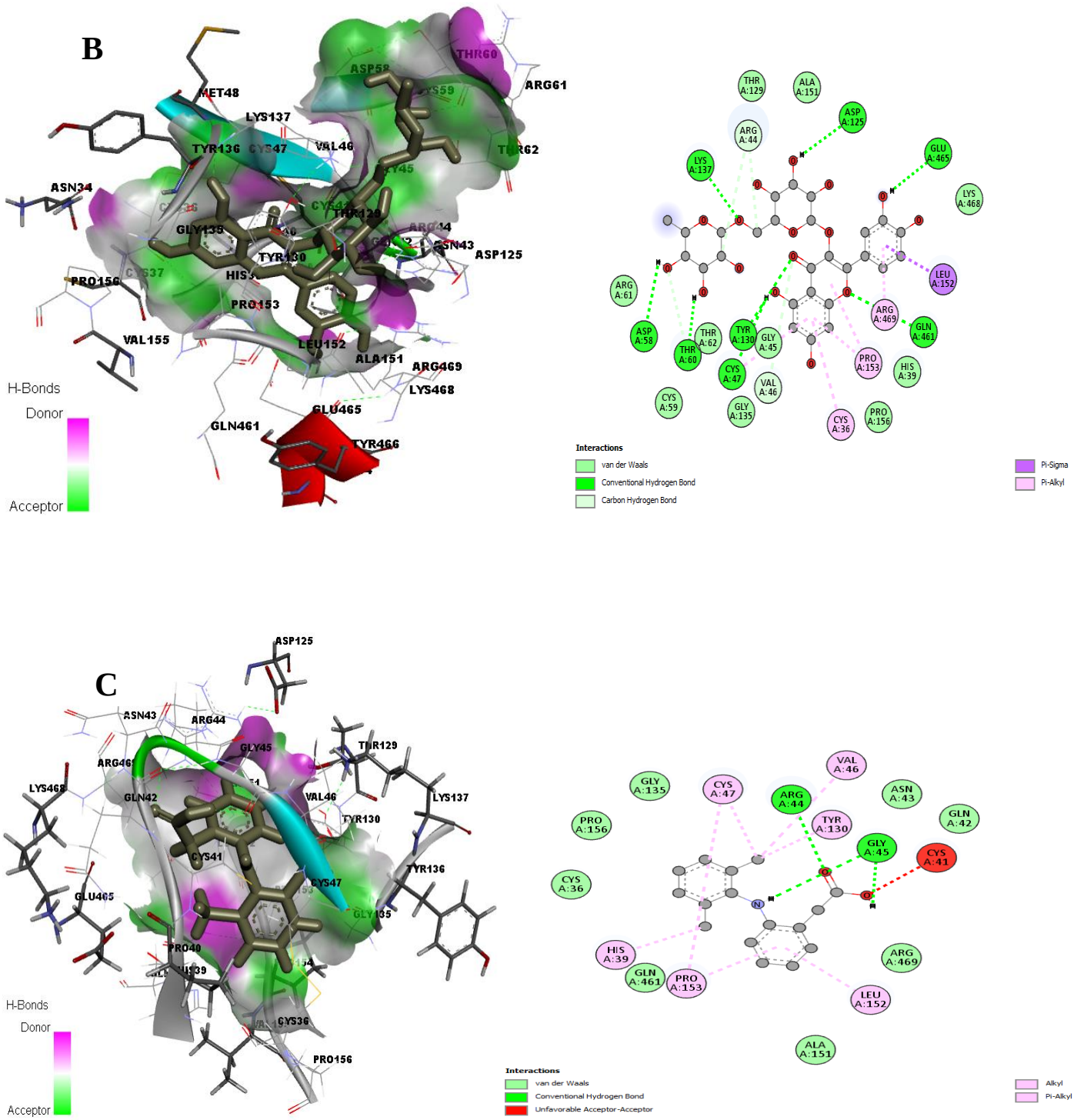

Figure 11 Molecular interactions of amino-acid residues of PTGS2 with A. Quercetin, B. Rutin and C. Diclofenac (standard drug) showing the 2D (right) and 3D (left) views

A. Quercetin binds firmly at the target site of PTGS2 with four conventional hydrogen bonds (CYS36, GLY45, TYR130 and GLU465), one carbon-hydrogen bond (VAL46), one pi-sigma bond (LEU152), two pi-alkyl bonds (CYS47 and PRO153) and twelve van der Waals forces. B. Rutin binds firmly at the target site of PTGS2 with eight conventional hydrogen bonds (CYS47, ASP58, THR60, GLN61, ASP125, TYR130, LYS137), three carbon-hydrogen bonds, one pi-sigma bond, three pi-alkyl bonds and ten van der Waals forces C. Diclofenac bind firmly at the target site of PTGS2 with two conventional hydrogen bonds (ARG44 and GLY45), six alkyl and pi-alkyl bonds and seven van der Waals forces.

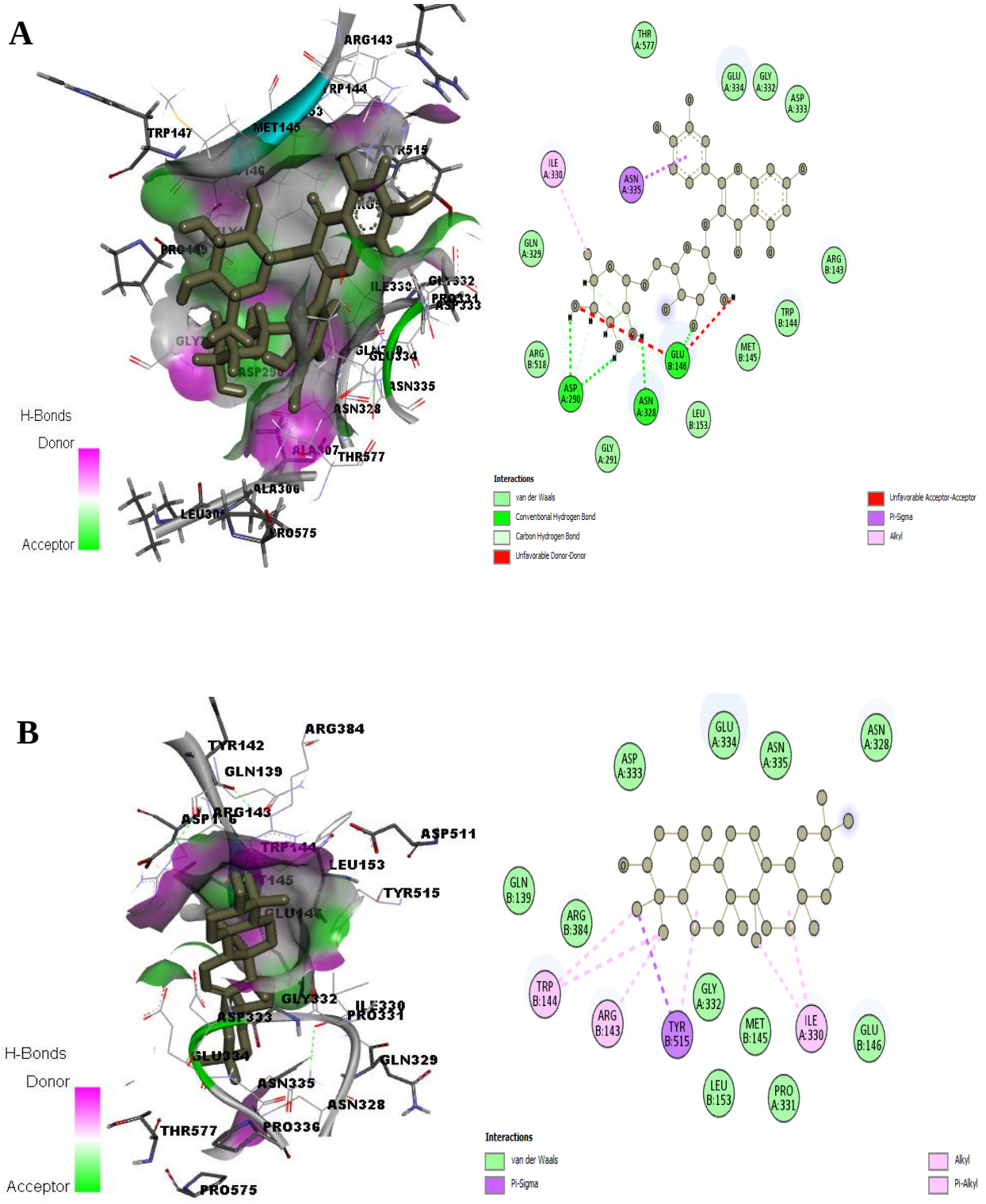

Figure 12 Molecular interactions of amino-acid residues of ALOX5 with A. Rutin and B. Beta-amyrin showing the 2D (right) and 3D (left) views

A. Rutin binds firmly at the target site of ALOX5 with four conventional hydrogen bonds (ARG101, GLN129, LYS133 and GLU134), one carbon-hydrogen bond (HIS130), one pi-pi T-shaped alkyl interaction (HIS130), pi-alkyl bonds with VAL110 and LYS133 and five van der Waals forces. B. Beta-amyrin binds at the target site of ALOX5 with three alkyl bonds (ARG143, TRP144 and ILE330), one pi-sigma bond (TYR515) and eleven van der Waals forces.

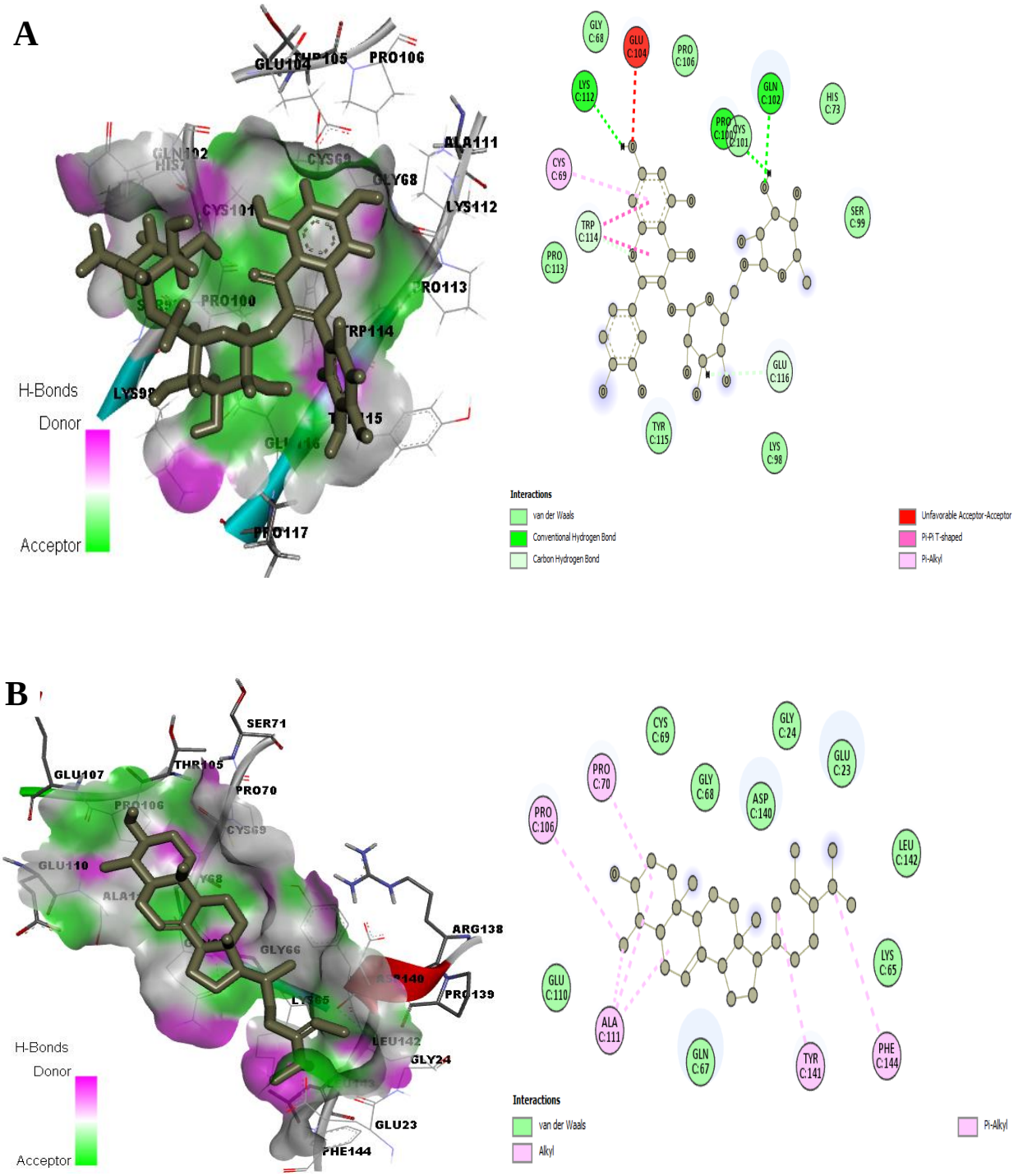

Figure 13 Molecular interactions of amino-acid residues of TNF-α with A. Rutin and Citrostadienol showing the 2D (up) and 3D (down) views

A. Ruin binds firmly at the target site of TNF-α with three conventional hydrogen bonds (PRO100, GLN102 and LYS112), pi-pi T-shaped bonds with TRP114, one pi-alkyl bond (CYS69) and nine van der Waals forces. Citrostadienol binds at the target site of TNF-α forming alkyl and alkyl interactions with five amino acids (PRO70, PRO106, ALA111, TYR141 and PHE144) and van der Waals forces with nine amino acids.

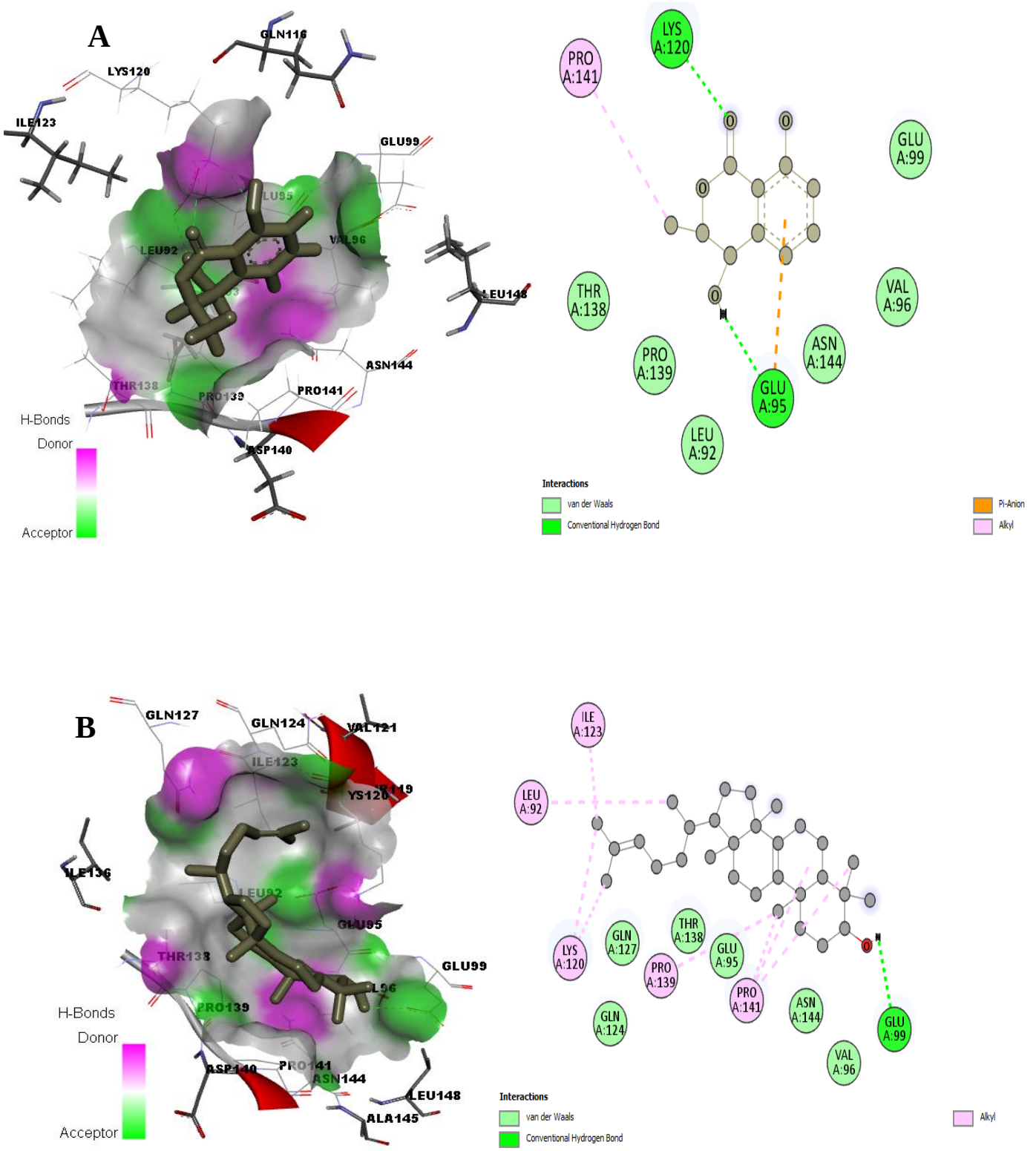

Figure 14 Molecular interactions of amino-acid residues of IL-6 with 4-hydroxymellein showing the 2D (right) and 3D (left) views. A. 4-hydroxymellein binds firmly at the target site of IL- with two conventional hydrogen bonds (GLU95 and LYS120), one pi-anion interaction with GLU95, one alkyl bond and six van der Waals forces. B. Tirucallol binds at the target site of IL-6 forming a hydrogen bond with GLU99, alkyl and alkyl interactions with five amino acids and van der Waals forces with six amino acids.

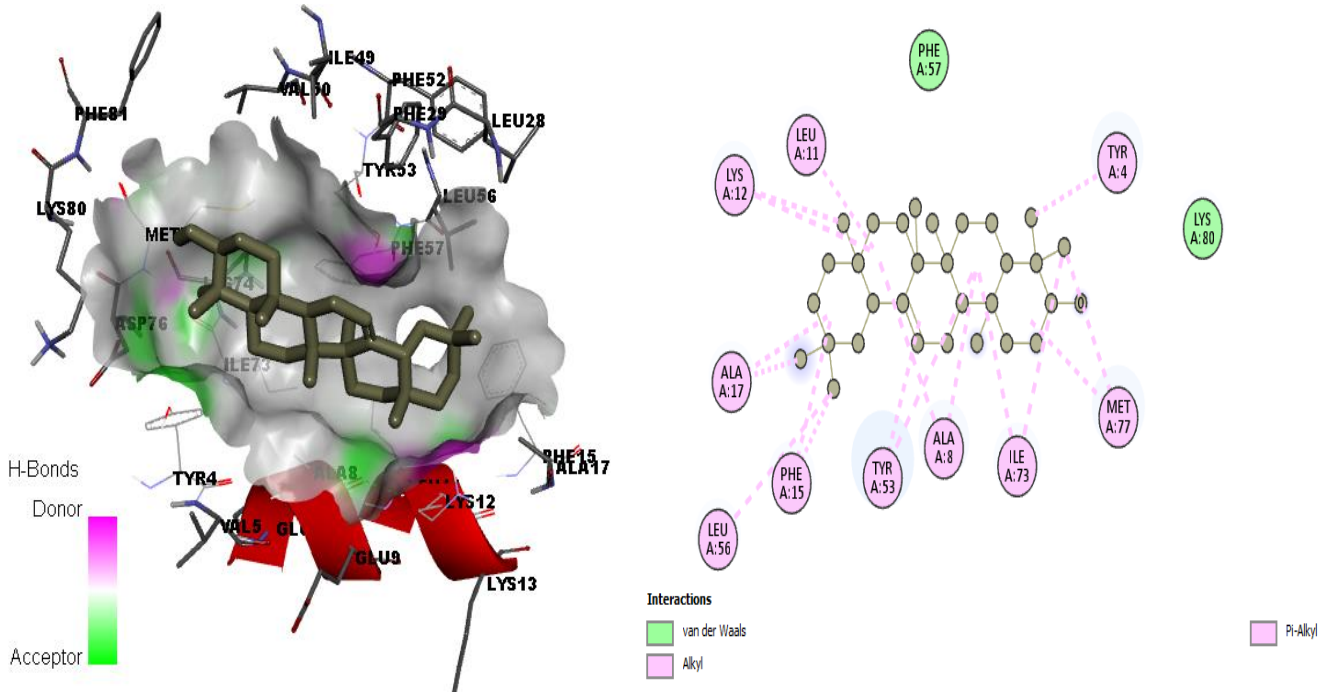

Figure 15 Molecular interactions of amino-acid residues of IFN-γ with beta-amyrin showing the 2D (right) and 3D (left) views Beta-amyrin binds at the target site of IFN-γ with ten alkyl and pi-alkyl bonds and two van der Waals forces (PHE57 and LYS80).

4. DISCUSSION

Uncontrolled inflammation could eventually result in disorders such as rheumatoid arthritis, psoriasis, periodontitis, inflammatory bowel disease and even cancers (Diakos et al., 2014). Non-steroidal anti-inflammatory drugs (NSAIDs) and corticosteroids are widely applied therapeutic agents which have achieved good therapeutic effects. Some side effects have however resulted the to their extensive use. Meanwhile, based on continuous breakthroughs in studies for compatibility of traditional medicine, increasing attention has been paid because of its significant therapeutic effects and minimal side effects (Li et al., 2019).

Several in vivo and in vitro studies on *Nigella sativa* and *Moringa oleifera* reveal that these plants possess anti-inflammatory activity (Chehl et al., 2009; Tshabalala et al., 2019). Although research on the anti-inflammatory potential of these plants continues, their molecular mechanism of action remains unclear. Fortunately, network pharmacology, which is especially suitable for multi-compound and multi-target analysis, provides a prospective method to solve this problem with bioinformatics, molecular biology and databases (Jiang et al., 2021).

In this study, network pharmacology and molecular docking were used to analyze the anti-inflammatory mechanism of *Nigella sativa* and *Moringa oleifera*. Network analysis predicted the modulation of ninety-eight inflammatory proteins by sixty-four phytoconstituents which suggests multiple compounds and protein interaction. Based on network pharmacology data, phytoconstituents, including rutin, beta-sitosterone, astragalin, beta-amyrin, quercetin and 4-hydroxymellein and other compounds are the most important nodes of the entire network. Previous studies have shown that rutin, beta-sitosterone, astragalin, beta-amyrin, quercetin and others, have an obvious anti-inflammatory effect (Yoo et al., 2014; Paniagua-Perez et al., 2017; Hu et al., 2020; Melo et al., 2011; Saeedi-Boroujeni and Mahmoudian-Sani, 2021). PTGS2, TNF-α, IL6 and NFKB1are the targets associated connected with inflammation-related pathways such as TNF and IL-17 signaling pathways. These results suggest that *N. sativa* and *M. oleifera* could probably regulate inflammation as well as the immune system. PTGS2, also known as COX-2 is an enzyme that catalyzes arachidonic acid to produce prostaglandins, thereby playing a pro-inflammatory role and unsettling the balance of the internal environment (Jain et al., 2015).

PTGS2 can be inhibited by inhibitors, thus blocking the conversion of arachidonic acid into prostaglandins, thus reducing the level of prostaglandins and alleviating inflammation and pain symptoms of tissues involved in prostaglandins (Zhang et al., 2011). TNF-α and IL-6 are pro-inflammatory cytokines that are involved in the upregulation of inflammatory reactions (Zhang and An, 2007). TNF-α can mediate inflammatory reactions, induce the production of IL-1β, IL-6 and other inflammatory factors and

aggravate the local inflammatory reaction (Turner et al., 2007). IL-6 is produced locally in the inflamed tissue following cellular activation by bacterial lipopolysaccharide or other cytokines such as IL-1β or TNF-α (Roshene and Ramesh, 2017). TNF-α is mainly secreted by activated T lymphocytes and mononuclear macrophages. On the other hand, IL6 is a signaling molecule that can be secreted by various cells of the body including, lymphocytes, macrophages/monocytes and epithelial cells (Zhu et al., 2021). NFKB1 (nuclear factor – kappa B1) also known as p50 is an inducible transcription factor that regulates a large number of genes involved in diverse processes of the immune and inflammatory responses (Liu et al., 2017).

The target levels of AKT1, HSP90AA1 and TNF-α were excessively expressed in the protein-protein interaction (PPI) network suggesting that they may play a pivotal role in the anti-inflammatory effects of *N. sativa* and *M. oleifera.* AKT1 (RAC-alpha serine/threonine-protein kinase) is a member of the AKT kinase family that regulates metabolism, proliferation, cell survival, gene expression, growth and angiogenesis through a series of downstream substrates (Tianyu and Liying, 2021). Studies reveal that AKT1 is essential for acute inflammation and exerts its effects primarily through the regulation of vascular permeability, leading to edema and leukocyte extravasation (Di Lorenzo et al., 2009). The heat shock protein 90α (HSP90α), encoded by the HSP90AA1 gene is a 90kDa ATP-dependent molecular chaperone that guides the late-stage tertiary folding and maintains the conformational integrity of multiple proteins such as oncogenic proteins, steroid receptors and transcription factors (Taipale et al., 2010).

HSP90 is widely expressed in eukaryotic cells but usually in a latent, uncomplexed form whereas tumors express high levels of catalytically active HSP90 found in complex with oncogenic client proteins. HSP90 is also highly expressed in inflammatory cells (Lilja et al., 2021). HSP90 inhibitors have been shown to ameliorate inflammatory and auto-immune diseases such as encephalomyelitis, rheumatoid arthritis and systemic lupus erythematosus (Tukaj and Wegrzyn, 2016). Similarly, thirty-three pathways were identified to be associated with proteins related to inflammation with reference to KEGG pathway analysis. The key targets were mainly concentrated in pathways such as the TNF signaling pathway, Human cytomegalovirus infection, and MAPK signaling pathway. The main proteins involved in these pathways include TNF-α, PTGS2, IL2, IL6, NFKB1, CASP3, and NFKBIA among others.

Furthermore, molecular docking technology was used to verify the core active components and target proteins on the prediction results of network pharmacology. The proteins F2, NR1H3, AKT1, HSP90AA1, IL2, NFKB1, PTGS2, ALOX5, TNF-α and IL6 were docked with the different compounds predicted by the network pharmacology. The verification results showed that the binding free energies of the compounds with the targets were much less than -5 Kcal/mol, which indicated that the ligand molecules could bind spontaneously (Abdullahi and Adeniji, 2020). To further validate the docking results, molecular docking was carried out between most of the compounds of *N. sativa* and *M. oleifera* and the aforementioned proteins in addition to IFN-γ (Interferon-gamma). The results showed that some of the compounds had lower binding affinities than the ones predicted by network pharmacology.

However, the compounds predicted by network pharmacology (apart from the interaction between rutin and PTGS2) interacted with more amino acid residues and formed more hydrogen bonds with the amino acid residues. Hydrogen bonds are important in protein-ligand interaction because they stabilize the ligand in the binding pocket (Kostal, 2016). Hydrogen bonds occur between a hydrogen atom's negatively charged groups (e.g., N, O, F). When several hydrogen bonds occur simultaneously at the binding site, they increase the strength and stability of drug-receptor interaction substantially. However, too many hydrogen bond donors/acceptors (like in the case of rutin and PTGS2 interaction) can have a deleterious effect on the drug's membrane partition and permeability. Too many hydrogen bonds can reduce the affinity toward the hydrophobic membrane region and increase the desolvation penalty upon penetration of the drug (Coimbra et al., 2021). All of this gives credence to the fact that the network pharmacology tool is effective in drug development.

IFN-γ also had a strong binding affinity with some of the compounds, including beta-amyrin (-10.7Kcal/mol), taraxerol (-10.1Kcal/mol) and hederagenin (-9.8Kcal/mol) among others. Drug-likeness character of each phytoconstituents from N. saiva and M. oleifera was predicted based on "Lipinski's Rule of Five" which is a qualitative assessment to evaluate the drug-like property concerning factors like oral bioavailability (Lipinski, 2004). In the present study, most of the compounds possess positive drug likeness scores reflecting their oral bioavailability. Similarly, the ADMET of each phytoconstituents was predicted to assess the important pharmacokinetic parameters in the human body including the probable toxicity of each molecule and was compared with diclofenac.

5. CONCLUSION

In conclusion, a network-based pharmacological analysis was utilized to predict the molecular targets for the anti-inflammatory activity of *Nigella sativa* and *Moringa oleifera.* Target proteins, including NR1H3, F2, AKT1, HSP90AA1, IL2, NFKB1, PTGS2, ALOX5,

TNF-α, IL6 and IFN-γ, as well as signaling pathways such as TNF, MAPK, IL-17 and HIF-1 were linked to the anti-inflammatory activity of *N. sativa* and *Moringa oleifera.* Based on network pharmacology data and molecular docking, phytoconstituents which include rutin, beta-sitosterone, astragalin, beta-amyrin and quercetin were predicted to inhibit key inflammatory proteins. These molecular targets may contribute to the overall anti-inflammatory activity of *N. sativa* and *M. oleifera* and its potential therapeutic applications for several inflammatory-mediated diseases.

Informed consent

Not applicable.

Ethical approval

Not applicable.

Conflicts of interests

The authors declare that there are no conflicts of interests.

Funding

The study has not received any external funding.

Data and materials availability

All data associated with this study are present in the paper.

REFERENCES AND NOTES

1. Abdullahi M, Adeniji SE. In-silico Molecular Docking and ADME/Pharmacokinetic Prediction Studies of Some Novel Carboxamide Derivatives as Anti-tubercular Agents. Chemistry Africa 2020; 3:989–1000. doi: 10.1007/s42250-020-00 162-3
2. Borquaye LS, Doetse MS, Baah SO, Mensah JA. Anti-inflammatory and anti-oxidant activities of ethanolic extracts of *Tamarindus indica L.* (Fabaceae). Cogent Chem 2020; 6:1-11. doi: 10.1080/23312009.2020.1743403
3. Chehl N, Chipitsyna G, Gong Q, Yeo CJ, Arafat HA. Antiinflammatory effects of the *Nigella sativa* seed extract, thymoquinone, in pancreatic cancer cells. HPB (Oxford) 2009; 11(5):373-381. doi: 10.1111/j.1477-2574.2009.00059.x
4. Coimbra JT, Feghali R, Ribeiro RP, Ramos MJ, Fernandes PA. The importance of intramolecular hydrogen bonds on the translocation of the small drug piracetam through a lipid bilayer. RSC Adv 2021; 11:899-908. doi: 10.1039/D0RA09995C
5. Di Lorenzo A, Fernández-Hernando C, Cirino G, Sessa WC. AKT1 is critical for acute inflammation and histamine-mediated vascular leakage. Proc Natl Acad Sci USA 2009; 106 (34):14552–14557. doi: 10.1073/pnas.0904073106
6. Duyu T, Khanal P, Khatib NA, Patil BM. *Mimosa pudica* Modulates Neuroactive Ligand Receptor Interaction in Parkinson's Disease. Indian J Pharm Educ 2020; 54(3):732-739. doi: 10.5530/ijper.54.3.124
7. Geremew H, Shibeshi W, Tamiru W, Engdawork E. Experimental evaluation of analgesic and anti-inflammatory activity of 80% methanolic leaf extract of *Moringa stenopetala* Bak. F. in mice. Ethiop Pharm J 2015; 31(1):15–26. doi: 10.4314 /epj.v31i1.2
8. Ghlichloo I, Gerriets V. Nonsteroidal Anti-inflammatory Drugs (NSAIDs). In: StatPearls [Internet]. Treasure Island (FL): StatPearls Publishing 2021.
9. Gogoi B, Gogoi D, Silla Y, Kakoti BB, Bhau BS. Network pharmacology-based virtual screening of natural products from *Clerodendrum* species for identification of novel anti-cancer therapeutics. Mol Biosyst 2017; 13(2):406-416. doi: 10.1 039/C6MB00807K
10. Gu J, Gui Y, Chen L, Yuan G, Lu HZ, Xu X. Use of Natural Products as Chemical Library for Drug Discovery and Network Pharmacology. PLoS One 2013; 8. doi: 10.1371/ journal.pone.0062839
11. Hannan MA, Rahman MA, Sohag A, Uddin MJ, Dash R, Sikder MH, Rahman MS, Timalsina B, Munni YA, Sarker PP, Alam M, Mohibbullah M, Haque MN, Jahan I, Hossain MT, Afrin T, Rahman MM, Tahjib-Ul-Arif M, Mitra S, Oktaviani DF, Khan MK, Choi HJ, Moon IS, Kim B. Black Cumin (*Nigella sativa L.*): A Comprehensive Review on Phytochemistry, Health Benefits, Molecular Pharmacology, and Safety. Nutrients 2021; 13(6):1784. doi: 10.3390/nu13061784
12. Hu X, Wang M, Pan Y, Xie Y, Han J, Zhang X, Niayele R, He H, Li Q, Zhao T, Cui Y, Yu S. Anti-inflammatory

effect of Astragalin and Chlorogenic acid on Escherichia coli-induced inflammation of sheep endometrial epithelium cells. Front Vet Sci 2020; 7(201):1-13. doi: 10.3389/fvets.2020.00201

13. Jain P, Pandey R, Shukla SS. Inflammation. In: Inflammation: Natural Resources and Its Applications. SpringerBriefs in Immunology. Springer, New Delhi 2015; 5-14. doi: 10.1007/97 8-81-322-2163-0_2
14. Jiang Q, Han L, Liu X, Zhang F. Anti-inflammatory properties of Fangji Huangqi Tang: Discovery based on network pharmacology, molecular docking and arrow smith tools. Res Sq 2021; 2(3):1-13. doi: 10.1016/j.phyplu.2022.100296
15. Johnson TO, Odoh KD, Nwonuma CO, Akinsanmi AO, Adegboyega AE. Biochemical evaluation and molecular docking assessment of the anti-inflammatory potential of *Phyllanthus nivosus* leaf against ulcerative colitis. Heliyon 2020; 6(5):e03893. doi: 10.1016/j.heliyon.2020.e03893
16. Kim S, Thiessen PA, Bolton EE, Chen J, Fu G, Gindulyte A, Han L, He J, He S, Shoemaker BA, Wang J, Yu B, Zhang J, Bryant SH. PubChem Substance and Compound databases. Nucleic Acids Res 2015; 44:D1202–13. doi: 10.1093/nar/gkv951
17. Kolodziejska J, Kolodziejczyk M. Diclofenac in the treatment of pain in patients with rheumatic diseases. Reumatologia 2018; 56(3):174-183. doi: 10.5114/reum.2018.76816
18. Kooti W, Hasanzadeh-Noohi Z, Sharafi-Ahvazi N, Asadi-Samani M, Ashtary-Larky D. Phytochemistry, pharmacology and therapeutic uses of black seed (*Nigella sativa*). Chin J Nat Med 2016; 14(10):732-745. doi: 10.1016/S1875-5364(16)30088-7
19. Kosala K, Widodo MA, Santoso S, Karyono S. In vitro and in vivo anti-inflammatory activities of *Coptosapelta flavescens* Korth root's methanol extract. J Appl Pharm Sci 2018; 8(9):42-48. doi: 10.7324/JAPS.2018.8907
20. Kostal J. Hydrogen bonding. Advances in Molecular Toxicology 2016; 10:139-186. doi: 10.1016/B978-0-12-804700-2. 00004-0
21. Kumar V, Abbas AK, Aster JC. Inflammation and Repair. In: Ribins Basic Pathology, 10th edn. Elsevier, Pennsylvania, USA 2018; 57-96.
22. Li SM, Li JG, Xu H. A New Perspective for Chinese Medicine Intervention for Coronary Artery Disease: Targeting Inflammation. Chin J Integr Med 2019; 25:3-8. doi: 10.1007/s11 655-018-2995-1
23. Lilja A, Weeden CE, McArthur K, Nguyen T, Donald A, Wong ZX, Dousha L, Bozinovski S, Vlahos R, Burns CJ, Asselin-Labat M, Anderson GP. HSP90 Inhibition Suppresses Lipopolysaccharide-Induced Lung Inflammation in vivo. Plos One 2015; 10(1):e0114975. doi: 10.1371/journal.pone.0114975
24. Lipinski CA. Lead and drug like compounds: The rule-of-five revolution. Drug Discov Today Technol 2004; 1(4):337-341. doi: 10.1016/j.ddtec.2004.11.007
25. Liu T, Zhang L, Joo D, Sun S. NF-κB signaling in inflammation. Sig Transduct Target Ther 2017; 2(17023). doi: 1 0.1038/sigtrans.2017.23
26. Mallenkuppe R, Homabalegowda H, Gouri MD, Basavaraju PS, Chandrashekharaiah UB. History, Taxonomy and Propagation of Moringa oleifera – A Review. SSR Inst. Int J Life Sci 2019; 5(3):2322-232. doi: 10.21276/SSR-IIJLS.2019.5.3.7
27. Melo CM, Morais TC, Tome AR, Brito GA, Chaves MH, Rao VS, Santos FA. Anti-inflammatory effect of α, β-amyrin, a triterpene from *Protium heptaphyllum*, on cerulein-induced acute pancreatitis in mice. Imflamm Res 2011; 60(7):673-681. doi: 10.1007/s00011-011-0321-x
28. Paniagua-Perez F, Flores-Mondragon G, Reyes-Legorreta C, Herrara-Lopez B, Cervantes-Hernandez I, Madrigal-Santillan O, Morales-Gonzalez JA, Alvarez-Gonzalez I, Madrigal-Bujaidar E. Evaluation of the anti-inflammatory capacity of beta-sitosterol in rodent assays. Afr J Tradit Complement Altern Med 2017; 14(1):123-130. doi: 10.21010/ajtcam.v14i1.13
29. Que W, Chen M, Yang L, Zhang B, Zhao Z, Liu M, Cheng Y, Qiu H. A network pharmacology-based investigation on the bioactive ingredients and molecular mechanisms of *Gelsemium elegans Benth* against colorectal cancer. BMC Complement Med Ther 2021; 21(99):1-18. doi: 10.1186/s12906-021-03273-7
30. Razis AF, Ibrahim MD, Kntayya SB. Health Benefits of *Moringa oleifera*. Asian Pac J Cancer Prev 2014; 15(20):8571-857 6. doi: 10.7314/apjcp.2014.15.20.8571
31. Roshene R, Ramesh A. Cytokines. J Pharm Sci Res 2017; 9(5):7 19-721.
32. Roth SH. Coming to terms with nonsteroidal anti-inflammatory drug gastropathy. Drugs 2012; 72:873-879. doi: 1 0.2165/11633740-000000000-00000
33. Saeedi-Boroujeni A, Mahmoudian-Sani. Anti-inflammatory potential of Quercetin in COVID-19 treatment. J Inflamm 2021; 18(3). doi: 10.1186/s12950-021-00268-6
34. Srivastava M, Dhakad PK, Srivastava B. A Review on Medicinal Constituents and Therapeutic Potential of *Moringa oleifera*. Univers J Plant Sci 2020; 8(2):22-33. doi: 10.13189/ujps .2020.080202
35. Taipale M, Jarosz DF, Lindquist S. HSP90 at the hub of protein homeostasis: emerging mechanistic insights. Nat Rev Mol Cell Biol 2010; 11:515–528. doi: 10.1038/nrm2918

36. Tian W, Chen C, Zhao J, Liang J. CASTp 3.0: Computed atlas of surface topography of proteins. Nucleic Acids Res 2018; 46 (W1):W363-W367. doi: 10.1093/nar/gky473
37. Tianyu Z, Liying G. Identifying the molecular targets and mechanisms of xuebijing injection for the treatment of COVID-19 via network pharmacology and molecular docking. Bioengineered 2021; 12(1):2274-2287. doi: 10.1080/21655979.20 21.1933301
38. Tshabalala T, Ncube B, Madala NE, Nyakudya TT, Moyo HP, Sibanda M, Ndhlala AR. Scribbling the cat: A case of the "miracle" plant, *Moringa oleifera*. Plants 2019; 8(510):1-23. doi: 10.3390/plants8110510
39. Tukaj S, Wegrzyn G. Anti-Hsp90 therapy in autoimmune and inflammatory diseases: A review of preclinical studies. Cell Stress Chaperones 2016; 21(2):213-218. doi: 10.1007/s12192-01 6-0670-z
40. Turner NA, Mughal RS, Warburton P, O'Regan DJ, Ball SG, Porter KE. Mechanism of TNFα-induced IL-1α, IL-1β and IL-6 expression in human cardiac fibroblasts: Effects of stains and thiazolidinediones. Cardiovasc Res 2007; 76(1):81-90. doi: 10.1 016/j.cardiores.2007.06.003
41. Xie W, Ji L, Zhao T, Gao P. Identification of transcriptional factors and key genes in primary Osteoporosis by DNA microarray. Med Sci Monit 2015; 21:1333-1344. doi: 10.12659/ MSM.894111
42. Yang L, Xiao-yue W, Xue-min W, Zi-tong G, Jian-ping H. Values, properties and utility of different parts of *Moringa oleifera*: An overview. Chin Herb Med 2018; 10(4):371-378. doi: 10.1016/j.chmed.2018.09.002
43. Ye XW, Deng YL, Xia LT, Ren HM, Zhang JL. Uncovering the mechanism of the effects of Paeoniae Radix alba on iron- deficiency anaemia through a network pharmacology- based strategy. BMC Complement Med Ther 2020; 20(1):130. doi: 10. 1186/s12906-020-02925-4
44. Yoo H, Ku S, Baek Y, Bae J. Anti-inflammatory effects of rutin on HMGB1-induced inflammatory responses in vitro and in vivo. Inflamm Res 2014; 63(3):197-206. doi: 10.1007/s00011-013-0689-x
45. Yu B, Ke X, Yuan C, Chen P, Zhang Y, Lin N, Yang Y, Wu H. Network Pharmacology Integrated Molecular Docking Reveals the Anti-COVID-19 Mechanism of Xingnaojing Injection. Natural Product Communications 2020; 15(12):1-12. doi: 10.1177/1934578X20978025
46. Yuan H, Ma Q, Cui H, Liu G, Zhao X, Li W, Piao G. How can synergism of traditional medicines benefit from network pharmacology? Molecules 2017; 22(7):E1135. doi: 10.3390/ molecules22071135
47. Zhang FC. Cyclooxygenase-2 specific inhibitors. Chin Pharm J 2011; 46(11):875-876.
48. Zhang Y, Xie Y, Yu B, Yuan C, Yuan Z, Hong Z, Wu H, Yang Y. Network Pharmacology Integrated Molecular Docking Analysis of Potential Common Mechanisms of Shu-Feng-Jie- Du Capsule in the Treatment of SARS, MERS and COVID-19. Nat Prod Commun 2020; 15(11):1-12. doi: 10.1177/1934578X20 972914
49. Zhou Z, Chen B, Chen S, Lin M, Chen Y, Jin S, Chen W, Zhang Y. Applications of network pharmacology in traditional Chinese medicine research. Evid Based Complement Alternat Med 2020; 2020(1646905):1-7. doi: 10.1155/2020/1646905
50. Zhu N, Hou J, Yang N. Network pharmacology integrated with experimental validation revealed the anti-inflammatory effects of *Andrographis paniculata*. Sci Rep 2021; 11:9752. doi: 1 0.1038/s41598-021-89257-6